The Early to Late Cretaceous (Albian–Cenomanian) transition in Putumayo, Colombia: a biostratigraphic and carbon isotope stratigraphic correlation for northwestern South America

Javier Luque [a] *, Jonatan Bustos [b] **, Manuel Páez-Reyes [b, c] **, Alejandro Beltrán-Triviño [b], Angie Rodríguez [b], Alexandra Delgado [d], Johan M. Sánchez [d], Julián Caraballo [b], Mikel A. López-Horgue [d] **

[a] Museum of Zoology, Department of Zoology, University of Cambridge, Downing Street, Cambridge CB2 3EJ, UK

[b] School of Applied Sciences and Engineering, EAFIT University, Medellin 050022, Colombia

[c] Servicio Geológico Colombiano, Bogotá, Colombia

[d] Geologia Saila, Faculty of Science and Technology, University of the Basque Country UPV/EHU, 48940 Leioa (Biscay), Basque Country, Spain

* Corresponding author.

** Contributed equally.

E-mail addresses: jl2351@cam.ac.uk (J. Luque), jabustoss@unal.edu.co (J. Bustos), manuel.paez@gmail.com (M. Paez-Reyes), mikel.lopezhorgue@ehu.eus (M.A. López-Horgue)

ABSTRACT

Despite the rich geological and paleontological record of Colombia, the Putumayo region near Ecuador remains one of the least explored regions in the equatorial Neotropics, mainly due to its thick vegetation, deep rock weathering, soil formation, and ground cover, geographic remoteness, and inaccessibility of well-exposed outcrops. This has resulted in limited comparisons with neighboring basins and thus the generation of more comprehensive biostratigraphic correlations with western and northern South America, as well as other paleobiogeographic regions (e.g., Tethys, Western Interior Seaway). Here, we present 67 occurrences of uppermost Lower Cretaceous to lowermost Upper Cretaceous ammonoids and other macrofossils (e.g., bivalves, decapod crustaceans, osteichthyan fish remains, plant remains), as well as a $\delta^{13}C_{org}$ chemostratigraphic curve derived from 105 samples from the middle Albian of the uppermost Caballos Formation and the upper Albian to lower Cenomanian lower Villeta Formation, collected *in situ* from a stratigraphic section exposed along the Mocoa–San Francisco Road, Putumayo, Colombia, here called the San Francisco section. The chemostratigraphic, carbon-isotope curve for the region shows a great similarity with the shape of the accepted curve for the late Albian Oceanic Anoxic Event 1d, which is characterized by a worldwide long positive $\delta^{13}C$ excursion anomaly. The new biostratigraphic and isotopic data serve as a point of reference to compare the Putumayo Basin with neighboring basins (e.g., Marañon Basin in Perú, Oriente Basin in Ecuador, Upper Magdalena Valley Basin in Colombia), and thus the generation of more comprehensive upper Lower Cretaceous and lower Upper Cretaceous biostratigraphic and chemostratigraphic correlations for northwestern South America.

Keywords: Biostratigraphy; Geochemistry; Lower Cretaceous; Paleontology; Upper Cretaceous; Villeta Formation

1. Introduction

The latest Early Cretaceous to the earliest Late Cretaceous (Albian–Cenomanian) transition coincides with a time of greenhouse conditions (Friedrich et al., 2012), biological turnover (Leckie et al., 2002; Watkins et al., 2005), the Oceanic Anoxic Event (OAE) 1d (Kennedy et al., 2004; Luciani et al., 2004; Bornemann et al., 2005), and changes in shallow and deep-marine water chemistry.

In northwestern South America, the Albian–Cenomanian transition is characterized by the deposition of organic-rich shales, limestones, and sandstones (Macellari, 1988; Villamil, 1998; Villamil and Pindell, 1998; Sarmiento-Rojas, 2019). These rocks are exceptionally well recorded in the Upper Magdalena Valley Basin of Colombia (Peña et al., 2002), the Putumayo Basin of Colombia (Mora et al., 1998), central Peru (Navarro-Ramirez et al., 2017), and the Oriente Basin of Ecuador (White et al., 1995). These rocks provide a nearly complete record of OAE1d and the Albian–Cenomanian transition in the tropical realm.

The Putumayo region, located in southwestern Colombia near the border with Ecuador, is key to understanding the regional geological evolution of northern South America (Fig. 1). Unfortunately, despite its rich geological and paleontological record and oil and gas production, the Putumayo Basin is one of the least studied areas compared to other neighboring basins. Thus, the knowledge of this basin's paleontology, biostratigraphy, lithostratigraphy, and geochemistry is limited.

Similar to the adjacent Upper Magdalena Basin, faunal and palynological events point to an Albian–Cenomanian age at the transition of the Caballos–Villeta formations in the Putumayo Basin (Etayo-Serna, 1994; Jaramillo and Rueda, 2004; Mora et al., 2010). Although some attempts have been made to correlate Albian–Cenomanian strata in northwestern South America using ammonoid biostratigraphy (Etayo-Serna, 1979; Etayo-Serna and Carrillo, 1996; Jaillard et al., 1997; Navarro-Ramirez et al., 2017), these correlations have been limited to age assignations based on the known ranges of ammonite genera of Europe and North America. Some of the South American ammonite taxa, however, are morphologically different from forms described elsewhere (Etayo-Serna, 1979), and given that endemism is common among ammonites, age correlation from extratropical faunas into the tropical domain may not be accurate in many cases, especially considering the paucity of studies examining low latitudes and how they compare to extratropical latitudes. In addition, most studies have focused on 3D preserved specimens in concretions, while impressions or compacted specimens from shale facies have been understudied.

Other stratigraphic tools that can assist in age determination of Cretaceous fossils include, for instance, chemostratigraphy (e.g., Wissler et al., 2004). Chemostratigraphic correlation using stable C isotopes helps correlate fine-grain rocks at global and local scales (Cramer and Jarvis, 2020).

In this study, we provide new biostratigraphic and carbon isotope data for the transition from the Caballos to the Villeta formations, aiming to develop a more robust temporal framework for the Albian–Cenomanian boundary for basins in northwestern South America and other parts of the world. Specifically, we focus on 1) the ammonoid record of the upper Albian–lower Cenomanian in a here described stratigraphic section of the Putumayo Basin of Colombia; 2) the stable carbon isotopic record (i.e., $\delta^{13}C_{org}$) of the uppermost Albian–lowermost Cenomanian; 3) determining the presence of the Albian–Cenomanian OAE1d in the Putumayo succession; and 4) correlate Putumayo sections with other sections in northwestern South America and other extratropical basins.

2. Geological setting

The Putumayo Basin (Fig. 1) is a foreland basin in southern Colombia, which is considered the northern extension of the Marañon (Perú) and Oriente (Ecuador) basins, located along the eastern flank of the Andean Cordillera (e.g., Sarmiento-Rojas, 2019). The stratigraphy of the Putumayo Basin can be described by three tectonostratigraphic megasequences separated by regional unconformities: i.e., the Pre-Cretaceous, Cretaceous, and Cenozoic megasequences (e.g., Gonçalves et al., 2002). Pre-Cretaceous rocks consist of Upper Triassic–Lower Jurassic volcaniclastic red beds (Motema Formation, Fig. 2), which is overlain by the uppermost Lower Cretaceous (Aptian–Albian) clastic deposits of the Caballos Formation (Fig. 2). The Cretaceous sedimentary cycle continued with a maximum transgression, represented by the late Albian to Santonian clastic and calcareous succession informally referred in the literature as the Villeta Formation (Fig. 2). The transgressive sequence ended during the early Campanian, which was followed by progradation of continental and relatively transitional deposits during the late Maastrichtian and early Paleocene (Arena N and Rumiyaco formations) (Fig. 2). During the Eocene, deposition in the basin was dominated by fluvial/alluvial sandstones and conglomerates (Pepino Formation, Fig. 2). During the Oligocene, lacustrine/fluvial shales, siltstones, and sandstones of the Orteguaza were deposited (Fig. 2). Later, the continental to transitional shales, sandstones, and conglomerates of the Orito-Belén and the Ospina formations were deposited from the late Oligocene to the early Pliocene. Ultimately, the area was covered by the coarse siliciclastic deposits of the Guamués and Caimán formations during the Pliocene and Quaternary (Fig. 2).

The tectonic evolution controlled the sedimentary infill of the Putumayo Basin since the Late Triassic–Early Jurassic, when the Motema Formation filled grabens formed in a back-arc setting (Casero et al., 1997). During the Aptian–Maastrichtian interval, the Caballos and Villeta formations accumulated in a broad and shallow epicontinental sea that extended throughout most of northwestern South America (e.g., Gonçalves et al., 2002; Sarmiento-Rojas, 2019). During this interval, regional relative sea-level changes and paleoceanographic events controlled the sedimentation in the basin (Villamil and Pindell, 1998). During the Maastrichtian–early Paleocene interval, the final accretion of the Western Cordillera caused an initial inversion of inherited Mesozoic normal faults and structuration of Campanian strata (Cooper et al., 1995; Cooney and Lorente, 2009). Contemporaneously, the uplifting of the Central

Cordillera caused a change in the sedimentation patterns, transitioning from the marine Villeta Formation to the continental Rumiyaco Formation.

The convergence between the Nazca and South America plates intensified during the early Paleocene–middle Eocene, generating the inversion of extensional normal faults and the development of thrust and back-thrust structures, which originated a second pulse of uplifting of the continental crust, followed by the subsequent deposition of the conglomerates of the Pepino Formation in the eastern foreland until the late Eocene (Casero et al., 1997; Córdoba et al., 1997). During the middle Eocene–Middle Miocene interval, uplift of the Central Cordillera continued (Cooper et al., 1995) and induced flexural subsidence of the lithosphere allowed for the deposition of the Orito-Belén and Ospina formations. Ultimately, the tectonic inversion of Pre-Cretaceous, Cretaceous, and Paleogene depocenters is associated with the uplifting of the Eastern Cordillera and the development of the sub-Andean foreland basins (Coletta et al., 1990; Cooper et al., 1995; Casero et al., 1997).

3. Materials and methods

3.1. Locality

The 67 ammonites and other macrofossils described in this study (Figs. 3–6) were collected *in situ* in a stratigraphic section cropping out along the Mocoa–San Francisco Road in the Putumayo Department, Colombia (Figs. 1, 2).

3.2. Materials

3.2.1. Macrofossils

Macrofossils used in this study are deposited at the 'Escuela de Ciencias Aplicadas e Ingeniería' EAFIT University, Medellín, Colombia, with acronyms and catalog numbers AGESS. The morphological study of 55 ammonoid samples in the study area allowed us to recognize 14 morphotypes and at least nine genera. The exact stratigraphic position of the samples is indicated in the stratigraphic column of the study area (Fig. 2, Fig. S1).

For the anatomical description of the ammonites, we followed the works by Klug et al. (2015) and Jain (2017), with an emphasis on the recognition of features such as type of umbilicum, type and direction of ribs, and type of ornamentation. The preservation of most ammonoid specimens studied here are laterally-compressed shells, which sometimes hinders a detailed discussion at the specific or even generic levels. However, features such as ornamentations, diameter of the shells, and umbilical dimensions, are well-preserved and allow confident taxonomical assignations in most cases. Based on the overall morphological characters discernible in these specimens, we compared them with records of ammonites from other localities in Colombia and worldwide, including the Upper Magdalena Valley Basin (UMVB) in Colombia (e.g., Etayo-Serna and Carrillo, 1996), Venezuela (e.g., Renz, 1982), the Oriente Basin, Ecuador (e.g., Tschopp, 1953; Bulot et al., 2005), Texas, United States (e.g., Kennedy et al., 1998b, 2005; Gale and Kennedy, 2020), Spain (e.g., López-Horgue et al., 1999, 2009), México (e.g., Moreno-Bedmar et al., 2014), Algeria (e.g., Kennedy, 2020), Kazakhstan (e.g., Kennedy, 2013), and Tunisia (e.g., Kennedy and Gale, 2015; Kennedy, 2020). The estimated stratigraphic ranges follow the works of Renz (1982), Owen and Mutterlose (2006), and Gale and Kennedy (2020) for Albian ammonites, and Wright et al. (1996), Villamil (1998), Moreno-Bedmar et al. (2014), Kennedy (2020), Kennedy et al. (1998a, 1998b), and Kennedy and Klinger (2011) for Cenomanian ammonites.

3.2.2. Rock samples

Forty-seven rock samples were hand-collected in surface, *in situ*, and fresh, from selected intervals of the Villeta Formation along the road cut for stable carbon-isotope analyses (see subsection 3.3.2. below).

3.3. Methods

3.3.1. Macrofossil preparation and imaging

Most macrofossils in this study, particularly those from the Villeta Formation, are preserved in mudstones as semi-flattened impressions (Figs. 3–5). No mechanical preparation was required. For photography, the specimens were coated with sublimated ammonium chloride before photography to enhance the relief of anatomical features and ornamentation. Thus, the specimens were imaged ‘dry’, rather than ‘wet’ (immersed under alcohol), the latter occasionally done for photographing compressed invertebrate fossils to enhance contrast. Specimens were imaged using a digital camera Canon EOS Rebel T6.

3.3.2. Stable carbon-isotope analysis

A $\delta^{13}C_{org}$ chemostratigraphic curve was constructed based on 105 samples (Figs. 2, 8, Table S1). $\delta^{13}C_{org}$ was measured in a Carlo Erba elemental analyzer coupled to a Delta V Advantage isotope ratio mass spectrometer (EA-IRMS) at the University of Florida Light Stable Isotope Mass Spec Laboratory, Gainesville, Florida. Before the isotopic analysis, 1 gram of powder rock was dissolved in centrifuge tubes with 1N HCl. Samples were re-filled with acid several times until inorganic carbon removal was complete. Decarbonated samples were rinsed in deionized water. Samples were then transferred into glass vials and dried in the oven for 48 hours at 70°C. On average, 200 micrograms of C were loaded in tin capsules and combusted at 1020°C. Analytical accuracy and precision were monitored based on repeated analysis (n = 62) of lab standards calibrated against the V-PDB standard. Precision was better than 0.1‰. Final isotopic compositions were corrected using the two-point correction method of Coplen et al. (2006).

4. Systematic paleontology

Phylum Mollusca Linnaeus, 1758
Class Cephalopoda Cuvier, 1797
Subclass Ammonoidea von Zittel, 1884
Order Ammonitida Hyatt, 1889
Suborder Ammonitina Hyatt, 1889
Superfamily Hoplitoidea Douvillé, 1890
Family Schloenbachiidae Parona and Bonarelli, 1896
Genus *Schloenbachia* Neumayr, 1875

Schloenbachia? sp.
(Fig. 5A, P)

Material: Two specimens, one with a maximum diameter of 70 mm (AGESS-P-0155-01) (Fig. 5A), and a smaller one with a diameter of 40 mm (AGESS-P-0155-12) (Fig. 5P).

Description: Involute coiling, with the umbilicus comprising about 25% of the shell diameter, which is less conspicuous in the smaller specimen. Fine ribbing and ventrolateral clavi are shared by both specimens; the umbilical bullate tubercle is prominent in the largest specimen. No keel observed.

Remarks: Colombian specimens are comparable in size and tuberculation to the involute and less ornamented forms of the genus *Schloenbachia* presented in Kennedy (2013). However, the ribbing is finer without flank tubercles, as in the Colombian specimens. *Mrhiliceras lapparenti* from Madagascar (Wright et al., 1996, fig. 117.2c, d) shows a similar fine ribbing but bears a less marked umbilical tuberculation. Nevertheless, its assignation to *Schloenbachia* is tentative until new comparable specimens are obtained. Its occurrence in Colombia could be somehow anomalous since this genus is only known from the Boreal Realm (e.g., occurrences in England, Germany, northern Iran) (Wilmsen and Mosavinia, 2011).

Family Engonoceratidae Hyatt, 1900

Genus *Engonoceras* Neumayr and Uhlig, 1881

Engonoceras? sp.

(Fig. 5C, D, H–J, M)

Material: Six specimens: AGESS-P-0155-03, -08, -11, -14, -15 and -21.

Description: Six fragmentary specimens each corresponding approximately to one-third of a whorl. All small sized, except for one specimen (AGESS-P-0155-03, Fig. 5C). Common characters are high, slightly conical umbilical tubercles and wide flexuous ribs with wider interspaces; primary ribs branch from the umbilical tubercle. In smaller specimens (Fig. 5D, H–J, M), all ribs are weak or absent at the lower flank, thickening towards the ventrolateral area where they show a claviform tubercle. The largest specimen figured (Fig. 5C) does not show a ventrolateral clavi, the ventral area looks unornamented (despite its lateral compression), and the ribs are less flexuous than in the smaller specimens.

Remarks: The ribbing type, coiling, and tuberculation is comparable to *Engonoceras*-like ornamentation. However, the lack of clear ventral areas and conspicuous suture lines make difficult a better determination. If compared to *Engonoceras* forms from the upper Albian to lower Cenomanian of Texas (e.g., Kennedy et al., 1998b, 2005), the Colombian specimens share a robust ribbing but at a smaller size.

Superfamily Acanthoceratoidea de Grossouvre, 1894

Family Brancoceratidae Spath, 1934

Subfamily Mojsisovicziinae Hyatt, 1903

Genus *Oxytropidoceras* Stieler, 1920

Subgenus *Oxytropidoceras* (*Venezoliceras*) Spath, 1925

Oxytropidoceras (*Venezoliceras*) sp.

(Fig. 3A–L, N–R)

Material: Sixteen specimens: AGESS-P-0156-06, -07, -10, -12, -13, -17, -18, and -20, AGESS-P-0166-05, -09, -10, and -16, AGESS-P-0169-03, -04, and -06.

Description: Involute coiling and substantial whorl height increment are observable in complete specimens (Fig. 3E). Ribbing is well marked, with a density of about 25 ribs per half a whorl. Ribs are flexuous, bifurcate from a conspicuous umbilical bullate tubercle (e.g., Fig. 3I), get broader in the upper flank, and bend adorally in the ventrolateral shoulder where they are elevated and show the gradual acquisition of a prominent ventrolateral claviform tubercle (e.g., Fig. 3C). Keel strong and elevated.

Remarks: Specimens AGESS-P-0166-09, -10, AGESS-P-0156-06, -10, -13, -18, and -20 show well-preserved flanks from the umbilical area to the keel; specimens AGESS-P-0156-07, -12, -17, AGESS-P-0166-05 and -16, AGESS-P-0169-03, -04, -06 are partial side remains that preserve some taxonomically-informative characters. Coiling, ribbing pattern, and the gradual acquisition of the ventrolateral tubercle make these specimens identifiable and included in the subgenus *Venezoliceras*. The partial specimens are comparable to the best-preserved ones: ribbing pattern, keel, and especially the growth of the ventrolateral tubercle, are characteristics observable among the specimens.

The well-marked ventrolateral tubercle of some specimens (Fig. 3C, I, K) and the ribbing pattern make the Colombian specimens comparable to *Oxytropidoceras* (*Venezoliceras*) *karsteni*, a species common in the upper Albian of Venezuela (Renz, 1982, pl. 17, figs. 2, 3).

Subgenus *Oxytropidoceras* (*Laraiceras*) Renz, 1968

Oxytropidoceras (*Laraiceras*) sp.

(Fig. 3S, T)

Material: One specimen: AGESS-P-0156-01, an almost complete shell with flanks well preserved.

Description: Coiling and high keel similar to those of *O.* (*Venezoliceras*) sp. described above. Dense ribbing in the first half whorl preserved, with flexuous ribs bifurcating from a subtle bullate umbilical tubercle, being broader towards the keel, and showing a conspicuous tuberculate shape at the ventrolateral shoulder. This ribbing becomes progressively wider towards the second half of the whorl, with alternating long and short as well as bifurcating ribs near the mid flank, where a lateral tubercle appears; the umbilical tubercle is sharper and ventrolateral clavate tubercle strong, in the last quarter of the whorl preserved.

Remarks: The subgenus *Laraiceras* shows more spaced ribs and mainly alternating ones from the inner whorls. The specimen described here is placed in this subgenus due to the developed trituberculate stage. The ribbing pattern at early growth stages with bifurcated ribs resembling *Venezoliceras* suggests that this specimen may be an early form of the subgenus.

Oxytropidoceras? sp.
(Fig. 3M)

Material: One specimen: AGESS-P-0159-08.

Description: Small specimen with a maximum 18 mm diameter, involute coiling, with an umbilicus comprising 20% of the shell diameter. Keel is high, and the ventral area looks fastigiate on the last half a whorl, with a row of progressively sharper and claviform tubercles developed on the ventrolateral margin. Smooth flanks evolving to very weak and spaced ribs on the last half a whorl.

Remarks: The well-formed ventrolateral tubercle, the high keel, and the coiling make this Colombian specimen comparable to species of the genus *Oxytropidoceras* (e.g., subgenus *Venezoliceras*). However, in these specimens, the tuberculated stage occurs later in the ontogeny, together with a well-marked ribbing. The development of sharp tubercles, the change of shape of the ventral area, and the mainly smooth flanks at a very small size indicate the fast acquisition of overall changing ornamentation early in ontogeny. Thus, this specimen could be considered a dwarf form.

Other features, such as crowded suture lines towards the end of the conch, would help to determine if this is a dwarf offshoot of *Oxytropidoceras*.

Subfamily Mortoniceratinae Douvillé, 1912

Genus *Mortoniceras* Meek, 1876

Subgenus *Mortoniceras* (*Mortoniceras*) Meek, 1876

Discussion: In a recent paper on upper Albian ammonites from North-East Texas, Gale and Kennedy (2020) discuss the differences between two lineages of mortoniceratines, one with the characters of the *vespertinum* species and the other composed of cosmopolitan forms allied to the *inflatum-rostratum* group, named *Mortoniceras* by previous authors. They propose using the genus *Mortoniceras* for the *vespertinum* group, while retaining the genus *Pervinquieria* for the other clade. Given the few mortoniceratine specimens from the Putumayo sections, we follow the terminology from the Treatise (Wright et al., 1996) until new Colombian material becomes available for a more in-depth discussion of their generic placement.

Mortoniceras (*Mortoniceras*) cf. *vespertinum*

(Fig. 4D)

2020 *Mortoniceras vespertinum* (Morton) – Gale and Kennedy, p. 30, pl. 11, figs. 7–9 (with synonymy).

Material: One specimen: AGESS-P-0166-04.

Description: Specimen with a maximum shell diameter of 32 mm preserved. Evolute coiling with umbilicus comprises about 40% of the shell diameter. More than the last half a whorl bearing sharp conical umbilical and broader-claviform ventrolateral tubercles gaining strength adorally. Ribs are weak, possibly due to preservation, but not well marked on the flank; they appear to be straight, with primaries and maybe secondaries at the end of the shell, but no branching is evident. The ventrolateral area bears a division of the tubercle at the end of the preserved whorl. Keel is only conspicuous in the last quarter of the whorl.

Remarks: Despite its preservation, coiling, ribbing style, and tubercle shape as well as arrangement are critical features observed in the innermost whorls of species of the *vespertinum* group. The lack of adult stages in the Colombian collection prevents additional determinations; however, it is comparable to the early growth stages at similar shell diameter observed in *vespertinum* specimens of North Texas (e.g., Gale and Kennedy, 2020, pl. 11, figs. 7–9).

Mortoniceras (*Mortoniceras*) sp.
(Fig. 4A–C)

Material: Two specimens: AGESS-P-0168, near half a whorl of what seems to be a partial body chamber (Fig. 4A, B), and AGESS-P-0169-02, a fragmentary upper flank (Fig. 4C).
Description: Specimen AGESS-P-0168 shows nearly 9 wide ribs (Fig. 4B) separated by similarly wide interspaces, with a shape suggesting an evolute coiling. Ribs are slightly flexuous, mainly primaries extending from the umbilical wall to the ventrolateral area, where they are broader but do not reach the keel; some secondaries arise from the lower flank. The umbilical bullate tubercle is high; the mid-flank tubercle is low, and the ventrolateral tubercle bullate is broader near the keel. Ribs show conspicuous spiral ridges. The other specimen, AGESS-P-0169-02, fits this description.
Remarks: Spiral ridges are a prominent feature of *Elobiceras*, but it is also observed in other mortoniceratines (e.g., subgenus *Mortoniceras* and *Deiradoceras*). A mid-flank tubercle separates these specimens from *Elobiceras* from bituberculated species of *Mortoniceras*. The trituberculation ribbing and coiling make the Colombian specimens comparable in form to the *inflatum* group. Coarse ribbed trituberculated forms have been described in Texas (e.g., Gale and Kennedy, 2020) and in Europe (e.g., López-Horgue et al., 1999), some of them with spiral ridges, but the fragmentary condition of the Colombian specimen prevents further discussion.

Genus *Algericeras* Spath, 1925

Algericeras sp.
(Fig. 5R–U)

Material: Four specimens: Three complete small specimens with a similar shell diameter of about 15 mm, AGESS-P-0155-17, -18, and -19, and one fragment comprising a third of a whorl, AGESS-P-0155-20.

Description: Umbilicus comprises less than 30% of the shell diameter. Considering their small size, the ribbing is well developed in the last whorl showing similar characteristics. Ribbing is dense, with about 30 flexuous ribs in the last half a whorl. Ribs are sharp and narrow, with narrower interspaces; primaries branch into two from a slightly bullate umbilical tubercle, projected adorally at the ventral area from the upper third of the flank, where they are the widest. Secondary ribs arise from at lower third of the flank. Keel is not well preserved due to compression, but it is conspicuous at different parts on the ventral end.

Remarks: Despite the moderate preservation of the Colombian specimens, their coiling, umbilical breadth, ribbing, and keel make them comparable to *Algericeras*. This genus comprises small, dwarf examples that show a developed ribbing at small shell diameters, such as the specimens described here. The Colombian specimens are comparable to the type specimens of *Algericeras bogharensis* Coquand, 1879, from the type locality in Northern Algeria and other related from Tunisia (e.g., Kennedy, 2020, pl. 12, figs. 1–15, pl. 13, figs. 6–8).

Subfamily Brancoceratinae Spath, 1934

Genus *Hysteroceras* Hyatt, 1900

Hysteroceras sp. 1

(Fig. 4I, J)

Material: Two specimens: AGESS-P-0166-12 and AGESS-P-0166-17.

Description: Both specimens are small, evolute, with an umbilicus around one-third of a 20 mm diameter. Sharp and dense ribbing, nearly 20 ribs in the last half whorl. Ribs are flexuous and look broader than interspaces; they extend from the umbilical area showing a sharp umbilical tubercle from which rib bifurcation can be observed, cross the flank, and become wider at the ventrolateral area sharply bending towards a low keel. In the last half of the whorl, there are some solitary ribs are intercalated between branching ones.

Remarks: The size, coiling, conservative ribbing, and sharp umbilical tubercle, are features shared by many species of *Hysteroceras*. Rib density, their flexuous shape, and the presence of a low keel in the late stage are features that can be seen in species like *H. carinatum* from Venezuela (e.g., Renz, 1982, pl. 11, figs. 9–11). However, Colombian specimens seem to be slightly less evolute and more comparable to Tethyan forms (e.g., López-Horgue et al., 2009, fig. 6D–F).

Hysteroceras sp. 2
(Fig. 4H, M)

Material: Two specimens: AGESS-P-0156-04 and AGESS-P-0167-01.
Description: Small-sized, with a shell diameter of 41 and 28 mm, respectively. Evolute coiling, with the umbilicus comprising 44% of the shell diameter in both specimens. Ribs well developed from the innermost observable parts, quite conservative throughout the shell, consisting of slightly flexuous sharp ribs, bearing a sharp umbilical tubercle from which ribs branch; ribbing looks not branched at the end of the shell in specimen 0156-04 (fig. 4H), with a conspicuous elevated venter without keel. Ventrolateral terminations do not show a prominent tubercle at any growth stage.
Remarks: Both specimens share similar coiling and ribbing. Thus, they are included in the same taxonomic determination. The smaller one is interpreted as a juvenile with continuously branched ribbing. The ribbing pattern, tuberculation, and size are compatible with those reported for species of *Hysteroceras*. Specimens are comparable to some species without keel at the end of the conch occurring in the upper Albian of Venezuela (e.g., Renz, 1982, pl. 11, fig. 12, pl. 12, fig. 3).

Hysteroceras? sp.
(Fig. 4G, K, L)

Material: Three specimens: AGESS-P-0156-19, -21, and AGESS-P-0158-06.
Description: Small conchs with shell diameters from 20 to 35 mm and wide umbilicus around 40% of the shell diameter, with a ribbing pattern similar to described *Hysteroceras*; keel is only partially visible at the early growth stage in one

specimen (i.e., AGESS-P-0156-21). Preservation prevents more refined taxonomic determinations.

Family Forbesiceratidae Wright, 1952

Genus *Forbesiceras* Kossmat, 1897

Forbesiceras? sp.

(Fig. 5F, G, K, L, N, O)

Material: Six specimens: Three fragmentary specimens partially showing the upper flank and the ventral area; AGESS-P-0155-04, -09, and -22, and three fragmentary specimens showing the coiling of the last preserved whorl; AGESS-P-0155-05, -07, and -10.

Description and remarks: Despite the preservation, the ribs broadening towards the venter and mainly developed in the upper flank, together with the ventrolateral clavi linked by a subtle rib crossing the venter, with delicate parallel striations (Fig. 5K), make these Colombian specimens comparable to specimens of the genus *Forbesiceras* (e.g., the Algerian *F. largilliertianum* in Kennedy, 2020, and the Tunisian *F. chevillei* in Kennedy and Gale, 2015).

Family Acanthoceratidae de Grossouvre, 1894

Subfamily Mantelliceratinae Hyatt, 1903

Genus *Graysonites* Young, 1958

Graysonites sp.

(Fig. 5B, E, Q)

Material: Three specimens: AGESS-P-0155-02 (one whorl preserved), AGESS-P-0155-06, and AGESS-P-0155-24 (both fragmentary, approximately half a whorl); all similar in size.

Description: Involute coiling with high whorl expansion; in the complete specimen, the umbilicus comprises less than 25% of a 25 mm shell diameter. Flexuous ribbing is better preserved in specimen 0155-06 with a conspicuous umbilical bullate tubercle that gives rise to primary ribs crossing the flank and showing well-marked inner and clavate outer ventrolateral tubercles. Secondary ribs between primaries do not reach the umbilical area, and the interspaces are of similar width. There is no clear rib branching except for specimen 0155-24.

Remarks: Although the ventral area is not observed due to poor preservation, the observed coiling, bullate umbilical tubercle, and the row of two ventrolateral tubercles are diagnostic features of the genus *Graysonites*. Specimens are comparable to similar size examples from Texas (Kennedy et al., 2005, figs. 27T, 28P, 29A, B), Mexico (Moreno-Bedmar et al., 2014, fig. 4), Tunisia (Kennedy and Gale, 2015, pl. 9, figs. 4, 8), and Algeria (Kennedy, 2020, pl. 22, fig. 7). Mexican specimens assigned to *Graysonites* sp. (e.g., Moreno-Bedmar et al., 2014) show a wider umbilicus and a likely less involute coiling but a comparable tuberculation. Colombian specimens show flexuous ribs as in the Algerian *Graysonites elegans* Kennedy, 2020.

Superfamily Turrilitoidea Gill, 1871

Family Hamitidae Gill, 1871

Genus *Hamites* Parkinson, 1811

Hamites sp.

(Fig. 4N–Q)

Material: Four specimens: AGESS-P-0156-02 and AGESS-P-0166-01, -02, -03.

Description: Coiling in one plane is observable in specimen AGESS-P-0156-02 (Fig. 4Q). This specimen corresponds to a juvenile with open plane spiral coiling changing to a more open shaft adorally; rectiradiate ribbing weak. The rest of the specimens are partial shafts with a very open curvature in two of them (Fig. 4N, P), all showing rectiradiate ribbing, with approximately equal width in ribs and interspaces. No conspicuous tubercles.

Remarks: Fragmentary hamitids are difficult to ascribe to a given genus or species. However, the Putumayo specimens compare well to open-coiled *Hamites* species based on their ribbing and open coiling. The juvenile specimen shows similar coiling as *Idiohamites* at the same growth stage, but the lack of tubercles prevents its assignation to this genus.

5. Results

5.1. Age of the ammonoid bearing intervals

We distinguish two ammonoid-bearing intervals in the Putumayo section with differentiated faunal composition. These two intervals are separated by a nearly 100-m-thick gap in the ammonoid succession, which is mainly due to poor outcrop exposition.

The lower ammonite-bearing interval extends from 153.5 to 170 m above the base of the section (Fig. 2, Fig. S1) and is dominated by brancoceratids and, to a lesser extent, hamitids. In this lower interval, we identified six ammonoid-bearing horizons (Fig. 2), showing the following faunal succession (lowest to highest): 1) *Hysteroceras* sp.; 2) *Oxytropidoceras*? sp.; 3) *Oxytropidoceras* (*Venezoliceras*) sp., *Hysteroceras* sp. 1, *Mortoniceras* (*Mortoniceras*) cf. *vespertinum*, and *Hamites* sp.; 4) *Hysteroceras* sp. 2.; 5) *Mortoniceras* (*Mortoniceras*) sp.; and 6) *Oxytropidoceras* (*Venezoliceras*) sp., *Oxytropidoceras* (*Laraiceras*) sp., *Hysteroceras* sp. 2, *Hysteroceras*? sp., *Mortoniceras* (*Mortoniceras*) sp. and *Hamites* sp. (Figs. 3, 4). This interval is of early late Albian age, based on the occurrences of the cosmopolitan genera *Hysteroceras* and *Hamites*, as well as the subgenera *Venezoliceras*, *Laraiceras*, and *Mortoniceras* (Fig. 7).

The upper ammonoid-bearing interval in the Putumayo section is the single stratigraphic horizon 271 m above the base of the section (Fig. 2, interval **7**). This level contains *Schloenbachia*? sp., *Engonoceras*? sp., *Forbesiceras*? sp., *Algericeras* sp., and *Graysonites* sp. (Fig. 5). This assemblage characterizes the lowermost Cenomanian. Other fossils, such as the osteichthyan fish remains (e.g., scales) and plant remains, are fragmentary or non-diagnostic to elaborate on their detailed systematic affinities. The decapod crustacean remains in this horizon are represented by two taxa: a single cheliped of an axiidean ghost shrimp (Fig. 6L), and abundant non-axiidean shrimp remains (e.g., antennae, pleons, caudal fans). While a more precise systematic placement is not possible now, it is worth mentioning that this is the first report of crustacean macrofossils from the Putumayo Basin.

5.2. Carbon isotope chemostratigraphy

The $\delta^{13}C_{org}$ record of the San Francisco stratigraphic section plotted against stratigraphic height shows a range of ~4‰ and is punctuated by a positive anomaly between 175 to 205 m. The magnitude of this isotopic anomaly is 2‰ and represents a distinctive carbon event within a long-lasting decrease of the isotopic values that start at the section's base and extend to the positive anomaly's base at 175 m. Above the isotopic anomaly, there are no substantial variations in the values of $\delta^{13}C_{org}$, which ranged around 27.5‰ from 205 m to the last part of the record at 270 m (Fig. 8).

6. Discussion

6.1. The upper Albian ammonoid association

The upper Albian ammonoid associations in the Putumayo region show typical elements from Venezuela (*Venezoliceras*, *Laraiceras*; e.g., Renz, 1982) and Texas (*Mortoniceras* (*M.*) cf. *vespertinum*; e.g., Gale and Kennedy, 2020). There are cosmopolitan taxa, such as *Hysteroceras* and *Hamites*, which are characteristic of shallow marine platforms of the Tethyan province extending from South America to Western Europe, North Africa, Madagascar, India, and Iran, during early Late Albian times (e.g., Owen and Mutterlose, 2006). *Venezoliceras* occurs in the fauna, and has been described from Western Europe (e.g., López-Horgue et al., 2009), Peru, Texas, Mexico, Africa, Madagascar, and Venezuela (Renz, 1982; Wright et al., 1996). In this study, we follow here the upper Albian ammonoid zonal scheme proposed for the Western Tethyan area (in Northern Spain, López-Horgue et al., 1999, 2009; and in Suriname, Owen and Mutterlose, 2006). This scheme is primarily based on the ranges of relatively abundant cosmopolitan brancoceratids of the genera *Hysteroceras* and *Mortoniceras*.

The Lower Cretaceous ammonite working group (the Kilian Group) proposed an upper Albian biozonation based on the phyletic evolution of mortoniceratines (Reboulet et al., 2011; Szives et al., 2024). However, certain mortoniceratine index species are scarce, and the framework needs revision (López-Horgue and Owen, 2024). *Hysteroceras* and other faunal elements are diagnostic for the lower part of the upper Albian (the former *M. inflatum* Zone of Spath, 1941). The transition to the uppermost Albian (to the former *Stoliczkaia dispar* Zone) is also debated. The occurrence of *M.* (*M.*) cf. *vespertinum* in Putumayo and of Tethyan elements in Texas are the basis for an attempt of correlation of the biozones from both areas and, in addition, it allows for the comparison between the Western Tethyan biozonation used here and the tentative biozonal correlation of North-East Texas with Western Europe proposed by Gale and Kennedy (2020) (Fig. 7).

In Texas, the first Zone of *Adkinsites bravoensis* zone is the lowest upper Albian ammonite zone, and contains *Hysteroceras varicosum* and *Deiradoceras* spp., which are also a common faunal element in the *Hysteroceras orbignyi* and *H. binum* Subzones in the Western Tethys (e.g., López-Horgue et al., 2009). The occurrence in Texas of the inoceramid *Actinoceramus sulcatus* atop the Kiamichi Formation (forma C, synonym of *A. sulcatus biometricus*; Kennedy et al., 1999), i.e., the top of *A. bravoensis* Zone (Gale and Kennedy, 2020, fig. 4), correlates with the transition to the *H. binum* Zone in Europe (e.g., see Gale and Owen, 2010, figs. 1–5). In Putumayo, the ammonite occurrences in the in the first two stratigraphic levels with ammonites are insufficient to give a precise biozone; therefore, this is provided by their stratigraphic order (underneath level 3, Fig. 2), as discussed below.

The *Elobiceras* (*Craginites*) *serratescens* Zone in Texas contains *Hysteroceras* cf. *varicosum* and *H.* cf. *binum*; the latter is the index marker of its homonym Subzone in the Tethys (e.g., Owen and Mutterlose, 2006). *Craginites* sp. is a component of the *H. choffati* Subzone in Northern Spain (López-Horgue et al., 2009). *Mortoniceras* (*M.*) *vespertinum* occurs in the upper part of the *Eopachydiscus marcianus* Zone of Texas above the *E.* (*C.*) *serratescens* Zone. At Putumayo *M.* (*M.*) cf. *vespertinum* occurs together with *Oxytropidoceras* (*Venezoliceras*) sp. and *Hysteroceras* sp. 1 in level 3, above the levels 1 and 2, which only contains *Hysteroceras*? sp. and *Oxytropidoceras*? sp. Levels 1 and 2 at Putumayo may lie below the transition from *H. choffati* to *M.* (*M.*) *inflatum* Zones (level 3, Fig. 2), corresponding to the *Hysteroceras varicosum* Zone without further precision (Figs. 2, 7). *Pervinquieria* (*P.*) *equidistans* Zone in Texas contains mortoniceratines with a clear mid-flank tubercle, which are a distinctive element of the *M.* (*M.*) *inflatum* Zone in Europe (e.g., Owen, 2012). *Mortoniceras* (*M.*) sp. possesses a conspicuous mid-flank tubercle occur in levels 5 and 6 at Putumayo, together with *Hysteroceras*? sp. and *H.* sp. 2 in level 6, indicating the lower *Mortoniceras* (*M.*) *inflatum* Zone (sensu Wiedmann and Owen (2001) and Owen (2012)) at least between 166 and 170 m (levels 5 and 6; Figs. 2, 7). Abundant *Oxytropidoceras* (*Venezoliceras*) sp. and *O.* (*Laraiceras*) sp. occur in level 6 at Putumayo, supporting a stratigraphically highest record of this genus and subgenus in Colombia.

6.2. The lower Cenomanian ammonoid association

Putumayo level 7 (Fig. 2) contains a diverse association of morphospecies typical of the Cenomanian in the Tethyan Realm. *Graysonites* is a genus whose type species comes from Texas. Yet, it was widespread during the early Cenomanian in Texas, California, Mexico, Brazil, Tunisia, Algeria, Japan, and Spain (e.g., Wright et al., 1996; Moreno-Bedmar et al., 2014; Kennedy, 2020). The Putumayo *Graysonites* specimens are comparable to Algerian forms. *Algericeras* sp. from Putumayo is similar to the Algerian specimens (Kennedy, 2020), with the genus characterizing the basal Cenomanian in Tunisia, Madagascar, and Mexico. *Schloenbachia* is a highly plastic form, which indicates a lower Cenomanian placement in Europe. The rest of the association is composed of *Forbesiceras*? sp. and *Engonoceras*? sp., both longer-ranging forms; the former ranges from the lowermost Cenomanian (*N. carcitanense* Subzone of the *M. mantelli* Zone) to the uppermost Cenomanian *M. geslinianum* Zone in Europe (Kennedy and Klinger, 2008), and the latter is a common element in the lower Albian to lower Cenomanian associations in Texas (e.g., Kennedy et al., 1998a, 1998b, 2005), and shows a broader occurrence in Europe, Algeria, Tunisia, Mexico, and Colombia.

6.3. The Albian–Cenomanian boundary in northwestern South America

The Albian–Cenomanian boundary at 100.5 Ma coincides not only with the boundary of the foraminifera zones *Parathalmanninella appenninica* and *Thalmanninella globotruncanoides*, but also with the first occurrence of the calcareous nannoplankton *Corollithion kennedyi* (Gale et al., 2020). In northwestern South America, the *Parathalmanninella appenninica* biozone has been recognized in rocks of the Querecual Formation consistent with upper Albian rocks in Eastern Venezuela (Crespo de Cabrera et al., 1999). The lower Cenomanian *Thalmanninella globotruncanoides* biozone has not been identified in northwestern South America, hampering the unequivocal assignation of rock formations to this stage.

In northwestern South America, specifically in Venezuela and Colombia, Renz (1982) and Villamil (1998) recognized that the lowermost part of the Cenomanian is hard to identify based on ammonites. This interpretation is consistent with seismic, stratigraphic, and paleontological evidence that indicates the presence of an unconformity between the Albian and Cenomanian in several basins of the northern Andes (Jaillard et al., 2000; Jaimes and de Freitas, 2006; Etayo-Serna, 2019).

Ammonites and foraminifera in the Upper Magdalena Valley Basin of Colombia, however, indicate that the Albian–Cenomanian boundary is present within the lower part of the "Shale y bancos con *Costagyra*" informal unit (Etayo-Serna and Carrillo, 1996; León Rodriguez, 2002). Similarly, ammonoid and bivalve faunas in Perú show that the Albian–Cenomanian boundary is identifiable in the central and northern parts of the country (Benavides-Cáceres, 1956; Navarro-Ramirez et al., 2017).

In the Putumayo region, there are very few paleontological reports, such as the works of Royo y Gómez (1942) and Cucalón and Camacho (1966), who mentioned the occurrences of some ammonoids ("Paleohoplitidae", *Oxytropidoceras multifidum*, *Neoplycticeras*? *subtuberculatum*, *Neophlycticeras rhombifera*, *Mortoniceras*, *Neophycticeras*) and bivalbes (*Corbula*, *Astarte*, *Pecten compressus*, *Inoceramus plicatus*, *Inoceramus labiatus*, *Exogyra squamata*). Unfortunately, none of these specimens has known stratigraphic contexts, and no illustrations of the material are available. The ammonoid-dominated macrofossil fauna from the Putumayo Basin here studied are mainly late Albian, with a possible early Cenomanian component stratigraphically above (Fig. 2). The disappearance of several genera and subgenera circumscribed to the Albian (e.g., *Oxytropidoceras*-like forms), and the appearance of specimens akin to *Schloenbachia*, *Forbesiceras*, *Graysonites*, *Algericeras*, suggest that the ammonoid faunas span the late Albian–early Cenomanian (Young, 1958; Kennedy and Wright, 1981; Kennedy and Klinger, 2008, 2011; Kennedy, 2013) (Figs. 2–7). The occurrence of the ammonoid genera *Oxytropidoceras*, *Mortoniceras*, and *Schloenbachia* suggest interconnection during the mid-Cretaceous of the Putumayo Basin with the Upper Magdalena Valley in Colombia and the Oriente Basin in Ecuador (Tschopp, 1953; Etayo-Serna and Carrillo, 1996; Bulot et al., 2005). The new fossil assemblage is a reference point for comparing neighboring basins (Fig. 1), thus generating more comprehensive biostratigraphic correlations for northwestern South America during the latest Early Cretaceous.

6.4. The Oceanic Anoxic Event 1d in the San Francisco section, Putumayo

The Albian–Cenomanian oceanic anoxic event (OAE1d), considered a minor OAE compared to other Cretaceous anoxic events (Jenkyns, 2010), has not yet been studied in detail. In contrast to the Aptian–Albian OAE1a and the Cenomanian–Turonian OAE2, the OAE1d event is thought to be triggered by monsoonal intensification and stratification of the water column rather than massive volcanism

(Matsumoto et al., 2022). This event is characterized by two prolonged 1‰ to 0.5‰ positive anomalies found in several organic and inorganic C-isotope records separated by a negative anomaly of 0.5‰ to 1‰ (Richey et al., 2018) (Fig. 8). The higher $\delta^{13}C$ value of the second positive anomaly of OAE1d broadly corresponds with the Albian–Cenomanian boundary and can be used as a geochemical fingerprint of the boundary.

The C-isotope profile of the San Francisco section starts with isotopic values of -26‰, then at 170 m, the isotopic composition starts building up and reaches a peak of -25‰ at 180 m. Above that point, the isotopic composition decreases to a new minimum of -27‰ at 208.5 m and then raises up for about 1‰ until the end of the section (Figs. 2, 8). The trends and overall shape of the isotopic curve are remarkably similar to other profiles from different basins around the world (Fig. 8). This correlation implies that the initial part of the Albian–Cenomanian boundary OAE1d is recorded at the transition between the Caballos Formation and the Villeta Formation in the Putumayo Basin as previously suggested for the Upper Magdalena Basin (Villamil, 1998). In addition, deposition of organic-rich hemipelagic limestones of the "Cálizas del Tetuán Limestone" Formation in the adjacent Upper Magdalena Basin indicates widespread deoxygenation of the water column across the Albian-Cenomanian boundary in Colombia (Villamil et al., 1999).

7. Conclusions

We report 67 new occurrences of upper Albian–lower Cenomanian (~105–96 Ma) ammonites, bivalves, decapod crustaceans, and other macrofossils from the Villeta Formation in Putumayo, Colombia. This time interval and geographic area are poorly known in northwestern South America due to limited exposure of rocks and apparent stratigraphic hiatuses between the upper Albian and the lower Cenomanian.

We recognize two stratigraphic intervals containing distinctive ammonite faunas. The lowermost interval includes six levels bearing ammonoids such as *Hysteroceras* spp., *Oxytropidoceras* sp., *O.* (*Venezoliceras*) sp., *O.* (*Laraiceras*) sp., *Mortoniceras* (*Mortoniceras*) cf. *vespertinum*, *M.* (*Mortoniceras*) sp., and *Hamites* sp., indicative of the upper Albian. In contrast, the uppermost interval includes one ammonoid-bearing level with *Schloenbachia*-like species, *Engonoceras*? sp., *Forbesiceras*? sp., *Algericeras* sp. and *Graysonites* sp., indicative of the lowermost Cenomanian.

These mid-Cretaceous ammonite assemblages fill a spatial and temporal gap in our understanding of the Putumayo Basin and its fossil record. These new records will facilitate future biostratigraphic correlations with neighboring basins in northwestern South America (e.g., Upper Magdalena Valley and Llanos basins in Colombia, Cuenca Oriente in Ecuador, Marañón Basin in Perú), as well as to other basins globally.

The new carbon isotope record obtained from Putumayo in southern Colombia provides an additional tool for correlating rock formations during the Albian–Cenomanian transition in the region. This record helps in reducing uncertainties related to age determinations based on biostratigraphy alone. The correlation observed between tropical and extratropical regions suggests the potential to develop a global stratigraphic scheme based on C_{org} isotope events. Notably, the positive carbon isotopic anomaly discovered in the latest Albian of the San Francisco section is a consistent indicator of the Oceanic Anoxic Event 1d (OAE1d). This anomaly can be interpreted as a response of the carbon cycle to the burial of organic carbon in large oceanic areas, similar to other Mesozoic OAEs.

Acknowledgements

This study was supported by the “Convocatoria para la Financiación de Proyectos de Investigación en Geociencias para el Sector de Hidrocarburos, número: 877”, by the Agencia Nacional de Hidrocarburos (ANH) and the Ministerio de Ciencia, Tecnología e Innovación de Colombia (Minciencias), grant No. 877-2021, as part of the AGESS project: “Astrocronología e Inversión Geoquímica aplicada a la identificación de ‘sweet spots’ en rocas generadoras de clase mundial: Formaciones La Luna y Villeta, cuencas Putumayo y Valle Medio del Magdalena, Colombia”, carried out by the Research Group Tectonics and Environmental Geology at the ‘Escuela de Ciencias Aplicadas e Ingeniería’, EAFIT University, Medellín, Colombia. This work is also a contribution to the Basque Government Research Group IT1485-22 and to the project of the Spanish Research System PID2019-105670GB I00/AEI/10.13039/501100011033 (MAL-H). Special thanks go to Andrés Cárdenas (EAFIT) for early discussions and suggestions, Laura Redondo and Cristian Valencia (EAFIT), and Camilo Rengifo for their assistance in the field, and to Osman Varol (UK) for edits on an earlier version of this manuscript. Our sincere thanks to Josep Antonio Bedmar-Moreno and Joshua Slattery for their valuable suggestions and feedback on an earlier version of this manuscript.

References

Benavides-Cáceres, V.E., 1956. Cretaceous system in northern Peru. Bulletin of the American Museum of Natural History 108 (4), 1–212.

Bornemann, A., Pross, J., Reichelt, K., Herrle, J.O., Hemleben, C., Mutterlose, J., 2005. Reconstruction of short-term palaeoceanographic changes during the formation of the Late Albian 'Niveau Breistroffer' black shales (Oceanic Anoxic Event 1d, SE France). Journal of the Geological Society 162 (4), 623–639.

Bornemann, A., Erbacher, J., Heldt, M., Kollaske, T., Wilmsen, M., Lübke, N., Huck, S., Vollmar, N.M., Wonik, T., 2017. The Albian–Cenomanian transition and Oceanic Anoxic Event 1d — an example from the boreal realm. Sedimentology 64 (1), 44–65.

Bulot, L.G., Kennedy, W.J., Jaillard, E., Robert, E., 2005. Late Middle-early Late Albian ammonites from Ecuador. Cretaceous Research 26 (3), 450–459.

Casero, P., Salel, J.F., Rossato, A., 1997. Multidisciplinary correlative evidences for polyphase geological evolution of the foothills of the Cordillera Oriental (Colombia). Proceedings of the VI Simposio Bolivariano, Cartagena, Colombia, pp. 100–118.

Coletta, B., Hebrard, F., Letouzey, J., Werner, P., Rudkiewicz, J.L., 1990. Tectonic style and crustal structure of the Eastern Cordillera (Colombia) from a balanced cross-section. In: Letouzey, J. (Ed.), Petroleum and Tectonics in Mobile Belts. Editions Technip, Paris, pp. 81–100.

Cooney, P., Lorente, M., 2009. A structuring event of Campanian age in western Venezuela, interpreted from seismic and palaeontological data. Geological Society, London, Special Publications 328, 687–703.

Cooper, M., Addison, F., Alvarez, R., Coral, M., Graham, R., Hayward, A., Howe, S., Martinez, J., Naar, J., Peñas, R., Pulham, A.J., Taborda, A., 1995. Basin development and tectonic history of the Llanos Basin, Eastern Cordillera, and middle Magdalena Valley, Colombia. AAPG Bulletin 79 (10), 1421–1443.

Coplen, T.B., Brand, W.A., Gehre, M., Gröning, M., Meijer, H.A., Toman, B., Verkouteren, R.M., 2006. New guidelines for $\delta^{13}C$ measurements. Analytical Chemistry 78 (7), 2439–2441.

Coquand, H., 1879. Études supplémentaires sur la paléontologie algérienne. Bulletin de l'Académie d'Hippone 15, 1–449.

Córdoba, F., Buchelli, F., Moros, J., Calderón, W., Guerrero, C., Kairuz, E.C., Magoon, L., 1997. Proyecto evaluación regional Cuenca del Putumayo — Definición de los sistemas petrolíferos. Ecopetrol, Internal Report, Bogotá, Colombia, 140 pp.

Cramer, B., Jarvis, I., 2020. Carbon isotope stratigraphy. In: Gradstein, F.M., Ogg, J.G., Ogg, G.M. (Eds.), Geologic Time Scale 2020. Elsevier, Amsterdam, Netherlands, pp. 309–343.

Crespo de Cabrera, S., Sliter, W.V., Jarvis, I., 1999. Integrated foraminiferal biostratigraphy and chemostratigraphy of the Querecual Formation (Cretaceous), eastern Venezuela. The Journal of Foraminiferal Research 29 (4), 487–499.

Cucalón, I., Camacho, R., 1966. Compilación geológica de la cuenca del Putumayo. Servicio Geológico Nacional (SGNC), Bogotá, Colombia, 18 pp.

Cuvier, G., 1797. Tableau élémentaire de l'histoire naturelle des animaux, Corps législatiff et de l'Institut national, place du carrousel, No. 66a. Paris (Baudouin), imprimeur, an 6 [1798], 710 pp.

de Grossouvre, A., 1894. Recherches sur la craie supérieure, 2, Paléontologie. Les ammonites de la craie supérieure. Mémoires du Service de la Carte Géologique Détaillée de la France 1893, 264 pp.

Douvillé, H., 1890. Sur la classification des Cératites de la Craie. Bulletin de la Société Géologique de France 18 (3), 275–292.

Douvillé, H., 1912. Évolution et classification des Pulchelliidés. Bulletin de la Société Géologique de France 11 (4), 285–320.

Etayo-Serna, F., 1979. Zonation of the Cretaceous of Central Colombia by Ammonites. Ministerio de Minas y Energia, Instituto Nacional de Investigaciones Geológico-Mineras, Bogotá, Colombia, 186 pp.

Etayo-Serna, F., 1994. Estudios Geológicos del Valle Superior del Magdalena. Universidad Nacional de Colombia, Departamento de Geociencias, Bogotá, Colombia 293 pp.

Etayo-Serna, F., 2019. Basin development and tectonic history of the Middle Magdalena Valley. In: Etayo-Serna, F. (Ed.), Estudios Geológicos y Paleontológicos sobre el Cretácico en la Región del Embalse del Río Sogamoso, Valle Medio del Magdalena. Compilacion de los Estudios Geologicos Oficiales en Colombia No. 23. Servicio Geológico Colombiano, Bogotá, Colombia, pp. 412–423.

Etayo-Serna, F., Carrillo, G., 1996. Bioestratigrafía del Cretácico mediante Macrofósiles en la Sección El Ocal, Valle Superior del Magdalena, Colombia. Geología Colombiana 20, 81–92.

Friedrich, O., Norris, R.D., Erbacher, J., 2012. Evolution of middle to Late Cretaceous oceans — a 55 my record of Earth's temperature and carbon cycle. Geology 40 (2), 107–110.

Gale, A.S., Kennedy, W.J., 2020. Upper Albian ammonites from North-East Texas. Revue de Paleobiologie 39, 1–139.

Gale, A.S., Owen, H.G., 2010. Introduction to the Gault. In: Young, J.R., Gale, A.S., Knight, R.I., Smith, A.B. (Eds.), Fossils of the Gault Clay. The Palaeontological Association, London, pp. 1–15.

Gale, A., Mutterlose, J., Batenburg, S., Gradstein, F., Agterberg, F., Ogg, J., Petrizzo, M., 2020. The Cretaceous Period. In: Gradstein, F.M., Ogg, J.G., Ogg, G.M. (Eds.), Geologic Time Scale 2020. Elsevier, Amsterdam, Netherlands, pp. 1023–1086.

Gill, T., 1871. Arrangement of the families of mollusks prepared for the Smithsonian Institution (Vol. 227). Smithsonian Institution, Washington, 49 pp.

Giorgioni, M., 2012. Long-and short-term changes in Tethyan oceanography and in global carbon cycling during Albian–Cenomanian time. PhD thesis, Eidgenössische Technische Hochschule (ETH) Zürich, Zürich, Switzerland, 165 pp.

Giorgioni, M., Weissert, H., Bernasconi, S.M., Hochuli, P.A., Keller, C.E., Coccioni, R., Petrizzo, M.R., Lukeneder, A., Garcia, T.I., 2015. Paleoceanographic changes during the Albian–Cenomanian in the Tethys and North Atlantic and the onset of the Cretaceous chalk. Global and Planetary Change 126, 46–61.

Gonçalves, F.T., Mora, C.A., Córdoba, F., Kairuz, E.C., Giraldo, B.N., 2002. Petroleum generation and migration in the Putumayo Basin, Colombia: insights from an organic geochemistry and basin modeling study in the foothills. Marine and Petroleum Geology 19 (6), 711–725.

Hyatt, A., 1889. Genesis of the Arietidae. Smithsonian Contributions to Knowledge 673. Smithsonian Institution, Washington, 238 pp.

Hyatt, A., 1900. Cephalopoda. In: von Zittel, K.A. (Ed.), Textbook of Palaeontology. Eastman, London and New York, pp. 502–592.

Hyatt, A., 1903. Pseudoceratites of the Cretaceous. Monographs of the United States, Vol. 44. Geological Survey, US Government Printing Office, Washington, 352 pp.

Jaillard, E., Caron, M., Dhondt, A., Ordoñez, M., Andrade, R., Bengtson, P., Bulot, L., Cappetta, H., Dávila, C., Díaz, R., 1997. Síntesis estratigráfica y sedimentológica del Cretáceo y Paleógeno de la cuenca oriental del Ecuador. Orstom-Petroproduccion eds, Quito, Ecuador, 164 pp.

Jaillard, E., Hérail, G., Monfret, T., Díaz-Martínez, E., Baby, P., Lavenu, A., Dumont, J.-F., Cordani, U., Milani, E., Campos, D., 2000. Tectonic evolution of the Andes of Ecuador, Peru, Bolivia and northern Chile. In: Cordani, U., Milani, E., Thomaz Filho, A., Campos, D. (Eds.), Tectonic Evolution of South America. 31st International Geological Congress, Rio de Janeiro, Brazil, pp. 481–559.

Jaimes, E., de Freitas, M., 2006. An Albian–Cenomanian unconformity in the northern Andes: Evidence and tectonic significance. Journal of South American Earth Sciences 21 (4), 466–492.

Jain, S., 2017. Cephalopoda, Fundamentals of Invertebrate Palaeontology. In: Jain, S. (Ed.), Fundamentals of Invertebrate Palaeontology: Macrofossils. Springer Geology, New Delhi, India, pp. 31–102.

Jaramillo, C., Rueda, M., 2004. Impact of biostratigraphy on oil exploration. Tercera Convención Tecnica de la ACGGP, Piedecuesta, Santander, Colombia, pp. 1–6.

Jenkyns, H.C., 2010. Geochemistry of oceanic anoxic events. Geochemistry, Geophysics, Geosystems 11 (3), 1–30.

Kennedy, W.J., 2013. On variation in *Schloenbachia varians* (J. Sowerby, 1817) from the Lower Cenomanian of western Kazakhstan. Acta Geologica Polonica 63 (4), 443–468.

Kennedy, W.J., 2020. Upper Albian, Cenomanian, and Upper Turonian ammonite faunas from the Fahdène Formation of Central Tunisia and correlatives in northern Algeria. Acta Geologica Polonica 70 (2), 147–272.

Kennedy, W.J., Gale, A.S., 2015. Upper Albian and Cenomanian ammonites from Djebel-Mhrila, Central Tunisia. Revue de Paleobiologie 34 (2), 235–361.

Kennedy, W.J., Klinger, H.C., 2008. Cretaceous faunas from Zululand and Natal, South Africa. The ammonite family Forbesiceratidae Wright, 1952. African Natural History 4, 117–130.

Kennedy, W.J., Klinger, H.C., 2011. Cretaceous faunas from Zululand and Natal, South Africa. The ammonite genus *Oxytropidoceras* Stieler, 1920. African Natural History 7 (1), 69–102.

Kennedy, W.J., Wright, C.W., 1981. *Euhystrichoceras* and *Algericeras*, the last Mortoniceratine ammonites. Palaeontology 24 (2), 417–435.

Kennedy, W.J., Cobban, W.A., Gale, A.S., Hancock, J.M., Landman, N.H., 1998a. Ammonites from the Weno Limestone (Albian) in Northeast Texas. American Museum Novitates 3236, 1–46.

Kennedy, W.J., Landman, N.H., Cobban, W.A., 1998b. Engonoceratid ammonites from the Glen Rose limestone, Walnut clay, Goodland limestone, and Comanche Peak limestone (Albian) in Texas. American Museum Novitates 3221, 1–40.

Kennedy, W.J., Gale, A.S., Hancock, J.M., Crampton, J.S., Cobban, W.A., 1999. Ammonites and inoceramid bivalves from close to the Middle-Upper Albian boundary around Fort Worth, Texas. Journal of Paleontology 73 (6), 1101–1125.

Kennedy, W., Gale, A., Lees, J., Caron, M., 2004. The global boundary stratotype section and point (GSSP) for the base of the Cenomanian Stage, Mont Risou, Hautes-Alpes, France. Episodes – Journal of International Geoscience 27 (1), 21–32.

Kennedy, W.J., Cobban, W.A., Hancock, J., Gale, A.S., 2005. Upper Albian and Lower Cenomanian ammonites from the Main Street Limestone, Grayson Marl and Del Rio Clay in northeast Texas. Cretaceous Research 26 (3), 349–428.

Klug, C., Korn, D., Landman, N.H., Tanabe, K., Baets, K.D., Naglik, C., 2015. Describing ammonoid conchs. In: Klug, C., Korn, D., De Baets, K., Kruta, I., Mapes, R. (Eds.), Ammonoid Paleobiology: from Anatomy to Ecology (Vol. 43). Springer, Berlin, Germany, pp. 3–24.

Kossmat, F., 1897. Untersuchungen uber die Sudindische Kreideformation. Beitrage zur Palaontologie und Geologie Osterreich-Ungarns und des Orients 11, 1–46.

Leckie, R.M., Bralower, T.J., Cashman, R., 2002. Oceanic anoxic events and plankton evolution: Biotic response to tectonic forcing during the mid-Cretaceous. Paleoceanography 17 (3), 13-11–13-29.

León Rodriguez, L., 2002. Estudio micropaleontológico y bioestratigráfico con base en foraminíferos planctónicos de las “Calizas del Tetuán, Grupo Villeta”. Unpublished BSc thesis, Valle Superior del Magdalena. Universidad Nacional de Colombia, Bogotá, Colombia, 279 pp.

Linnaeus, C., 1758. Systema Naturae per Regna Tria Naturae, Secundum Classes, Ordines, Genera, Species, cum Characteribus, Differentiis, Synonymis, Locis, Laurentii Salvii, Holmiae, 532 pp.

López-Horgue, M.A., Owen, H.G., 2024. Western Pyrenees): New records, new taxa and their taxonomic and biostratigraphical value. Cretaceous Research 158, 105855.

López-Horgue, M.A., Owen, H.G., Rodriguez-Lázaro, J., Orue-Etxebarria, X., Fernández-Mendiola, P.A., García-Mondéjar, J., 1999. The late Albian–lower Cenomanian stratigraphic succession near Estella-Lizarra (Navarra, central northern Spain) and its regional and interregional correlation. Cretaceous Research 20, 369–402.

López-Horgue, M.A., Owen, H.G., Aranburu, A., Fernández-Mendiola, P.A., García-Mondéjar, J., 2009. Early late Albian (Cretaceous) of the central region of the Basque-Cantabrian basin, northern Spain: biostratigraphy based on ammonites and orbitolinids. Cretaceous Research 30, 385–400.

Luciani, V., Cobianchi, M., Jenkyns, H.C., 2004. Albian high-resolution biostratigraphy and isotope stratigraphy: the Coppa della Nuvola pelagic succession of the Gargano Promontory (Southern Italy). Eclogae Geologicae Helvetiae 97, 77–92.

Macellari, C.E., 1988. Cretaceous paleogeography and depositional cycles of western South America. Journal of South American Earth Sciences 1 (4), 373–418.

Matsumoto, H., Coccioni, R., Frontalini, F., Shirai, K., Jovane, L., Trindade, R., Savian, J.F., Kuroda, J., 2022. Mid-Cretaceous marine Os isotope evidence for heterogeneous cause of oceanic anoxic events. Nature Communications 13 Article number 239, doi: 10.1038/s41467-021-27817-0.

Meek, F.B., 1876. A report on the invertebrate Cretaceous and Tertiary fossils of the upper Missouri Country. Report of the United States Geological Survey of the Terrtories, Government Printing Office, Washington, 629 pp.

Mora, A., Mantilla, M., De Freitas, M., 2010. Cretaceous paleogeography and sedimentation in the Upper Magdalena and Putumayo Basins, southwestern Colombia. Search and Discovery Article 50246, 15–18.

Mora, J.A., Venegas, D., Vergara, L., 1998. Estratigrafía del Cretácico Superior y Terciario inferior en el sector norte de la Cuenca del Putumayo, departamento del Caquetá, Colombia. Geología Colombiana 23 (1), 31–77.

Moreno-Bedmar, J., Latil, J.-L., Villanueva-Amadoz, U., Calvillo-Canadell, L., Cevallos-Ferriz, S., 2014. Ammonite age-calibration of the EL Chango Fossil-Lagerstätte, Chiapas state (SE Mexico). Journal of South American Earth Sciences 56, 447–453.

Navarro-Ramirez, J., Bodin, S., Consorti, L., Immenhauser, A., 2017. Response of western South American epeiric-neritic ecosystem to middle Cretaceous Oceanic Anoxic Events. Cretaceous Research 75, 61–80.

Nederbragt, A.J., Fiorentino, A., Klosowska, B., 2001. Quantitative analysis of calcareous microfossils across the Albian–Cenomanian boundary oceanic anoxic event at DSDP Site 547 (North Atlantic). Palaeogeography, Palaeoclimatology, Palaeoecology 166 (3–4), 401–421.

Neumayr, V.H.M., 1875. Die Ammoniten der Kreide und die Systematik der Ammonitiden. Zeitschrift der Deutschen geologischen Gesellschaft 27, 854–942.

Neumayr, V.H.M., Uhlig, V., 1881. über Ammonitiden aus den Hilsbildungen Norddeutschlands. Palaeontographica 27 (3–6), 129–203.

Owen, H.G., 2012. The Gault Group (Early Cretaceous, Albian) in East Kent, S. E. England; its lithology and ammonite biozonation. Proceedings of the Geologists' Association 123, 742–765.

Owen, H.G., Mutterlose, J., 2006. Late Albian ammonites from off-shore Suriname-implications for biostratigraphy and palaeobiogeography. Cretaceous Research 27, 717–727.

Parkinson, J., 1811. The Fossil Starfish, Echini, Shells, Insect, Amphibia, Mammalia &c. Organic remains of a former world an examination of the mineralized remains of the vegetables and nimals of the antediluvian world; generally termed extraneous fossils (3a ed.). J. Robson, London, 455 pp.

Parona, C.F., Bonarelli, G., 1896. Fossili Albiani d'Escragnolles, del Nizzardo e della Liguria occidentale. Paleontographia Italica: Memorie di Paleontologia 2, 53–112.

Peña, J.J., Annicchiarico, G.P., Jaramillo, J.M., Velásquez, E., 2002. Las Calizas de Tetuan: una nueva unidad litoestratigrafica para la Subcuenca de Neiva, Valle Superior del Magdalena. Estratigrafia, petrografia y ambiente sedimentario. Revista de la Academia Colombiana de Ciencias Exactas, Fisicas y Naturales 26 (101), 481–497.

Reboulet, S., Rawson, P.F., Moreno-Bedmar, J.A., Aguirre-Urreta, M.B., Barragán, R., Bogomolov, Y., Company, M., González-Arreola, C., Idakieva Stoyanova, V., Lukeneder, A., Matrion, B., Mitta, V., Randrianaly, H., Vasicek, Z., Baraboshkin, E.J., Bert, D., Bersac, S., Bogdanova, T.N., Bulot, L.G., Latil, J.-L., Mikhailova, I.A., Ropolo, P., Szives, O., 2011. Report on the 4th International Meeting of the IUGS Lower Cretaceous Ammonite Working Group, the "Kilian Group" (Dijon, France, 30th August 2010). Cretaceous Research 32, 786–793.

Renz, O., 1968. Über die Untergattungen *Venezoliceras* Spath und *Laraiceras* n . subgen. der Gattung *Oxytropidoceras* Stieler (Ammonoidea) aus den Venezolanischen Anden. Eclogae Geologicae Helvetiae 61, 615–655.

Renz, O., 1982. The Cretaceous Ammonites of Venezuela. Birkhäuser Verlag, Basel, Switzerland, 132 pp.

Richey, J.D., Upchurch, G.R., Montañez, I.P., Lomax, B.H., Suarez, M.B., Crout, N.M., Joeckel, R., Ludvigson, G.A., Smith, J.J., 2018. Changes in CO_2 during Ocean Anoxic Event 1d indicate similarities to other carbon cycle perturbations. Earth and Planetary Science Letters 491, 172–182.

Royo y Gómez, J., 1942. Datos para la geología económica de Nariño y Alto Putumayo: Informe No. 313, Compilación de estudios geológicos oficiales en Colombia. Ministerio de Minas y Petróleos, Bogotá, Colombia, pp. 53–260.

Sarmiento-Rojas, L.F., 2019. Cretaceous stratigraphy and paleo-facies maps of northwestern South America. In: Cediel, F., Shaw, R.P. (Eds.), Geology and Tectonics of Northwestern South America: The Pacific-Caribbean-Andean Junction. Springer International Publishing, Cham, pp. 673–747.

Scotese, C.R., 2016. Tutorial: PALEOMAP paleoAtlas for GPlates and the paleoData plotter program. PALEOMAP Project, availabe at : http://www.earthbyte.org/paleomap-paleoatlas-for-gplates/.

Spath, L.F., 1925. On Upper Albian Ammonoidea from Portuguese East Africa, with an appendix on Upper Cretaceous ammonites from Maputoland. Annals of the Transvaal Museum 11 (3), 179–200.

Spath, L.F., 1934. A Monograph of the Ammonoidea of the Gault. Part XI. Monographs of the Palaeontographical Society 86 (390), 443–496.

Spath, L.F., 1941. A Monograph of the Ammonoidea of the Gault. Part XIV. Monographs of the Palaeontographical Society 95 (422), 609–668.

Stieler, V.C., 1920. Über sogenannte Mortoniceraten des Gault. Zentralblatt far Mineralogie, Geologie und Paláontologie 1920, 345–352.

Szives, O., Moreno-Bedmar, J.A., Aguirre-Urreta, B., Company, M., Frau, C., López-Horgue, M., Pictet, A., Ploch, I., Salazar, C., Barragán, R., Latil, J.-L., Lehmann, J., Robert, E., Reboulet, S., 2024. Report on the 7th International Meeting of the IUGS Lower Cretaceous Ammonite Working Group, the Kilian Group (Warsaw, Poland, 21st August 2022): State of the art on the current Standard Ammonite Zonation of the Western Tethyan Mediterranean Province. Cretaceous Research 153, 105716.

Takashima, R., Nishi, H., Yamanaka, T., Orihashi, Y., Tsujino, Y., Quidelleur, X., Hayashi, K., Sawada, K., Nakamura, H., Ando, T., 2019. Establishment of Upper Cretaceous bio- and carbon isotope stratigraphy in the northwest Pacific Ocean and radiometric ages around the Albian/Cenomanian, Coniacian/Santonian and Santonian/Campanian boundaries. Newsletters on Stratigraphy 52 (3), 341–376.

Tschopp, H.J., 1953. Oil Explorations in the Oriente of Ecuador, 1938–1950. American Association of Petroleum Geologists Bulletin 37 (10), 2303–2347.

Villamil, T., 1998. Chronology, relative sea-level history and new sequence stratigraphic model for basinal Cretaceous facies of Colombia. In: Pindell, J.L., Drake, C. (Eds.), Eustasy and Tectonostratigraphic Evolution of Northern South America. SEPM Special Publication 58, 161–216.

Villamil, T., Pindell, J.L., 1998. Mesozoic paleogeographic evolution of northern South America: Foundations for sequence stratigraphic studies in passive margin strata deposited during non-glacial times. In: Pindell, J.L., Drake, C. (Eds.), Eustasy and Tectonostratigraphic Evolution of Northern South America. SEPM Special Publication 58, 283–318.

Villamil, T., Arango, C., Hay, W.W., Barrera, E., Johnson, C.C., 1999. Plate tectonic paleoceanographic hypothesis for Cretaceous source rocks and cherts of northern South America, evolution of the Cretaceous Ocean-Climate System. Geological Society of America 332, 191–202.

von Zittel, K.A., 1884. Cephalopoda. In: Eastman, C.R. (Ed.), Handbuch der Paläontologie 1 (2). R. Oldenbourg, München/Leipzig, Germany, pp. 329–522.

Watkins, D.K., Cooper, M.J., Wilson, P.A., 2005. Calcareous nannoplankton response to late Albian oceanic anoxic event 1d in the western North Atlantic. Paleoceanography 20 (2), 1–14.

White, H.J., Skopec, R.A., Ramirez, F.A., Rodas, J.A., Bonilla, G., 1995. Reservoir characterization of the Hollin and Napo formations, western Oriente Basin, Ecuador. AAPG Memoir 62, 573–596.

Wiedmann, J., Owen, H.G., 2001. Late Albian ammonite biostratigraphy of the Kirchrode I borehole, Hannover, Germany. Palaeogeography, Palaeoclimatology, Palaeoecology 174, 161–180.

Wilmsen, M., Mosavinia, A., 2011. Phenotypic plasticity and taxonomy of *Schloenbachia varian*s (J. Sowerby, 1817) (Cretaceous Ammonoidea). Paläontologische Zeitschrift 85, 169–184.

Wissler, L., Weissert, H., Buonocunto, F.P., Ferreri, V., D'Argenio, B., 2004. Calibration of the Early Cretaceous time scale: a combined chemostratigraphic and cyclostratigraphic approach to the Barremian–Aptian interval, Campania Apennines and southern Alps (Italy). In: D'Argenio, B., Fischer, A.G., Premoli Silva, I., Weissert, H., Ferreri, V. (Eds.), Cyclostratigraphy: Approaches and Case Histories. SEPM (Society for Sedimentary Geology), Tulsa, Oklahoma, pp. 123–133.

Wright, C.W., 1952. A classification of the Cretaceous ammonites. Journal of Paleontology 26 (2), 213–222.

Wright, C.W., Calloman, J.H., Howart, M.K., 1996. Cretaceous Ammonoidea. Treatise on Invertebrate Paleontology, Part L, Mollusca 4, Revised. Geological Society of America, Boulder, Colorado, and University of Kansas Press, Lawrence, Kansas, 362 pp.

Young, K., 1958. *Graysonites*, a Cretaceous ammonite in Texas. Journal of Paleontology 32 (1), 171–182.

Figure captions

Fig. 1. Location map of the study area (white star indicates the studied Albian–Cenomanian strata), and general map of Colombia, showing the distribution of Cretaceous-only rocks and depocenters (modified after Sarmiento-Rojas, 2019).

Fig. 2. Litho-and biostratigraphy of the uppermost Lower Cretaceous to lowermost Upper Cretaceous in the Putumayo region, Colombia, northern South America. (A) Generalized lithostratigraphic column of the units in the study area. (B) Lithostratigraphic column of the middle to upper Albian–lower Cenomanian interval of the Villeta Formation at the Mocoa–San Francisco section (this study), showing the associated $\delta^{13}C_{org}$ chemostratigraphic curve and the stratigraphic ranges of ammonoids and other macrofossil occurrences (e.g., bivalves, decapod crustacean remains, osteichthyan fish remains). An expanded, detailed stratigraphic column is included in Fig. S1. Abbreviations: Alb-Cen? = Albian–Cenomanian? interval; Fm. = Formation; Gr. = Group; sp. = species indet.

Fig. 3. Upper Albian ammonites of the Villeta Formation, Putumayo, Colombia. (A–L, N–R) *Oxytropidoceras* (*Venezoliceras*) sp. (A, B, D, F) Specimens showing a keel; (A) AGESS-P-0169-03, two individuals, the smallest one showing the ventral side (bottom right), and the largest is an external mold in lateral view (upper left); (B) AGESS-P-0156-12, lateral view of the left side; (D) AGESS-P-0156-10, lateral view of the right side; (F) AGESS-P-0169-04, lateral view of the right side. (C, H–L, N–R) Specimens showing a keel and ribs bearing ventrolateral clavi; (C) AGESS-P-0156-17, lateral view of the right side; (H) AGESS-P-0166-10, lateral view of the left side; (I, J) AGESS-P-0156-06, lateral view (I) and counterpart (J) of right side; (K) AGESS-P-0156-07, lateral view of the right side; (L) AGESS-P-0156-18, lateral view of the right side; (N, O) AGESS-P-0166-16, lateral view of the counterpart (N) and part (O) of right side; (P) AGESS-P-0169-06, lateral view of the right side; (Q) AGESS-P-0166-09, external mold in lateral view of the right side; (R) AGESS-P-0156-20, lateral view of the right side. (E, G) Most complete specimens, showing the involute coiling of the last preserved whorl; (E) AGESS-P-0156-13, lateral view of the left side; (G) AGESS-P-0166-05, external mold in lateral view of the right side. (M) *Oxytropidoceras*? sp., AGESS-P-0159-08, small specimen showing the involute coiling of the last preserved whorl and ventrolateral tubercles. (S, T) *Oxytropidoceras* (*Laraiceras*) sp., AGESS-P-0156-01, showing a keel and three rows of tubercles (umbilical, low lateral, and ventrolateral) bearing on the long ribs, the ventrolateral tubercle has a clavus-like shape in its inner and outer terminations; lateral view of the counterpart (S) and part (T) of right side.

Fig. 4. Upper Albian ammonites of the Villeta Formation, Putumayo, Colombia. (A–C) *Mortoniceras* (*Mortoniceras*) sp. (A, B) AGESS-P-0168, lateral view of the counterpart (A) and part (B) of right side, showing trituberculate ribs. (C) AGESS-P-0169-02, external mold in lateral view of the right side. (D) *Mortoniceras* (*Mortoniceras*) cf. *vespertinum*, AGESS-P-0166-04, external mold in lateral view of the right side showing two rows of tubercles. (E, F) Aptychi showing articulate preservation of the two halves; (E) AGESS-P-0156-22; (F) AGESS-P-0156-23. (G, K, L) *Hysteroceras*? sp. small specimens showing evolute coiling of the last preserved whorl; (G) AGESS-P-0156-19, external mold in lateral view of the left side; (K) AGESS-P-0156-21, external mold in lateral view of the left side; (L) AGESS-P-0158-06, external mold in lateral view of the left side. (H, M) *Hysteroceras* sp. 2, small specimens showing evolute coiling of the last preserved whorl; (H) AGESS-P-0156-04, external mold in lateral view of the right side; (M) AGESS-P-0167-01, external mold in lateral view of the right side. (I, J) *Hysteroceras* sp. 1, small specimens showing evolute coiling of the last preserved whorl; (I), AGESS-P-0166-17, lateral view of the left side; (J) AGESS-P-0166-12, lateral view of the right side. (N–Q) *Hamites* sp. (N–P) Fragmentary specimens showing single radial ribs; (N) AGESS-P-0166-01, external mold; (O) AGESS-P-0166-02, external mold; (P) AGESS-P-0166-03, external mold. (Q) AGESS-P-0156-02, early whorls showing a crioconic coiling and fine radial ribs.

Fig. 5. Lower Cenomanian ammonites of the Villeta Formation, Putumayo, Colombia. (A, P) *Schloenbachia*? sp.; (A) AGESS-P-0155-01, external mold in lateral view of the right side, showing coiling of the last preserved whorl and umbilical tubercles; (P) AGESS-P-0155-12, lateral view of the left side, showing fine ribbing and ventrolateral clavi. (B, E, Q) *Graysonites* sp. showing three rows of tubercles (umbilical, inner- and outer- ventrolateral); (B) AGESS-P-0155-02, external mold in lateral view of the right side; (E) AGESS-P-0155-06, external mold in lateral view of the right side; (Q) AGESS-P-0155-24, external mold in lateral view of the left side. (C, D, H–J, M) *Engonoceras*? sp. showing slightly conical umbilical tubercles and wide flexuous ribs; (C) AGESS-P-0155-03, lateral view of the right side; (D) AGESS-P-0155-08, lateral view of the right side; (H) AGESS-P-0155-14, lateral view of the left side; (I) AGESS-P-0155-15, lateral view of the left side; (J) AGESS-P-0155-21, lateral view of the right side; (M) AGESS-P-0155-11, lateral view of the

right side. (F, G, K, L, N, O) *Forbesiceras*? sp. (F, K, O) Specimens showing ribs bearing ventrolateral clavi; (F) AGESS-P-0155-09, lateral view of the left side; (K) AGESS-P-0155-04, oblique view showing the upper part of the flank and the ventral area; (O) AGESS-P-0155-22, ventral view. (G, L, N) Specimens showing coiling of the last preserved whorl; (G) AGESS-P0155-10, lateral view of the right side; (L) AGESS-P-0155-05, lateral view of the right side; (N) AGESS-P0155-07, lateral view of the left side. (R–U) *Algericeras* sp., small specimens showing numerous fine ribs strongly project in the ventrolateral region; (R) AGESS-P-0155-17, external mold in lateral view of the right side; (S) AGESS-P-0155-18, external mold in lateral view of the left side; (T) AGESS-P-0155-19, lateral view of the left side; (U) AGESS-P-0155-20, external mold in lateral view of the left side.

Fig. 6. Middle Albian and upper Albian–lower Cenomanian macrofossils of the Caballo and Villeta formations in the San Francisco section, Putumayo, Colombia. (A–E, G) ?middle Albian bivalves of the Caballos Formation; (A) AGESS-P-0175-05, bivalve indet.; (B) AGESS-P-0175-04, *Buchotrigonia* sp., left valve; (C) AGESS-P-0161, Lophinae indet.; (D) AGESS-P-0175-06, bivalve indet.; (E) AGESS-P-0175-02, bivalve indet.; (G) AGESS-P-0175-03, bivalve indet. (F, H, K, L) Upper Albian macrofossils of the Villeta Formation; (F) AGESS-P-0169-05, bivalve indet.; (H) AGESS-P-0170-03, bivalve indet.; (K) AGESS-P-0169-01, leaf fragment of fern? indet.; (L) AGESS-P-0170-02, decapod crustacean propodus of cheliped, possibly of a callianassid shrimp. (I, J) Lower Cenomanian osteichthyan fish scales of the Villeta Formation; (I) AGESS-P-0155-26; (J) AGESS-P-0155-25.

Fig. 7. Biostratigraphic correlation of the upper Albian ammonites of the Putumayo area with the zonation of the Tethyan province, Northeast Texas, and Western Europe (López-Horgue et al., 2009; Gale and Kennedy, 2020). The association *Mortoniceras* (*Mortoniceras*) cf. *vespertinum*, *Oxytropidoceras* (*Venezoliceras*) sp., and *Hysteroceras* sp. 1 of level 3 (in red) is located in the transition of the *Hysteroceras choffati* to *Mortoniceras* (*Mortoniceras*) *inflatum* Zones. The association of the *Mortoniceras* (*M.*) sp. and *Hysteroceras* spp. in level 6 (in red) is probably in the lower *Mortoniceras* (*M.*) *inflatum* Zone.

Fig. 8. Carbon-isotope chemostratigraphic correlation across the Albian–Cenomanian boundary between the San Francisco Section (Putumayo, Colombia) and five other globally-distributed sections. (A) $\delta^{13}C_{org}$ of the San Francisco section, Colombia (equatorial Atlantic realm; this work). (B) $\delta^{13}C_{org}$ of Uchucchacua, Peru (eastern Pacific; Navarro-Ramirez et al., 2017). (C) $\delta^{13}C_{org}$ of Monte Petrano, Italy (Tethys realm; Giorgioni, 2012; Giorgioni et al., 2015). (D) $\delta^{13}C_{org}$ of the Yezo Group, Japan (Pacific realm; Takashima et al., 2019). (E) $\delta^{13}C_{carb}$ of the Mazagan Plateau (Tethys realm; Nederbragt et al., 2001). (F) $\delta^{13}C_{carb}$ of Anderten, Germany (Boreal realm; Bornemann et al., 2017). C-isotope excursions are correlated based on foraminifera zones (FZ), macrofossil regional zonations (MZ), and nannoplankton zones (NZ) that define the Albian–Cenomanian boundary interval (ACBI). The red dot dashed lines represent the approximate position of the Albian–Cenomanian boundary (ACB). The dashed line represents correlatable peaks or troughs in the C-isotope record. Red line curves for all sections are three-point moving averages of the data, except for the section of the Mazagan Plateau (E), based on the raw data and not averaged. Paleogeographic map reconstruction after Scotese (2016).

Fig. S1. Detailed lithostratigraphic column of the Lower to Upper Cretaceous (Albian–Cenomanian) section studied in the Mocoa–San Francisco road (i.e., San Francisco section), Department of Putumayo, Colombia, northern South America.

Table

Table S1. List of Lower to Upper Cretaceous macrofossils (ammonoids, bivalves, crustacean remains, osteichthyan fish remains, plant remains) from the middle–upper Aptian to lower Cenomanian Caballos and Villeta formations in the Mocoa–San Francisco section, Putumayo region, Colombia, northern South America). Stratigraphic heights as in Fig. 2 and Fig. S1.

Figure 1

Click here to access/download;Figure;Figure 1_Location Map_RR.jpg

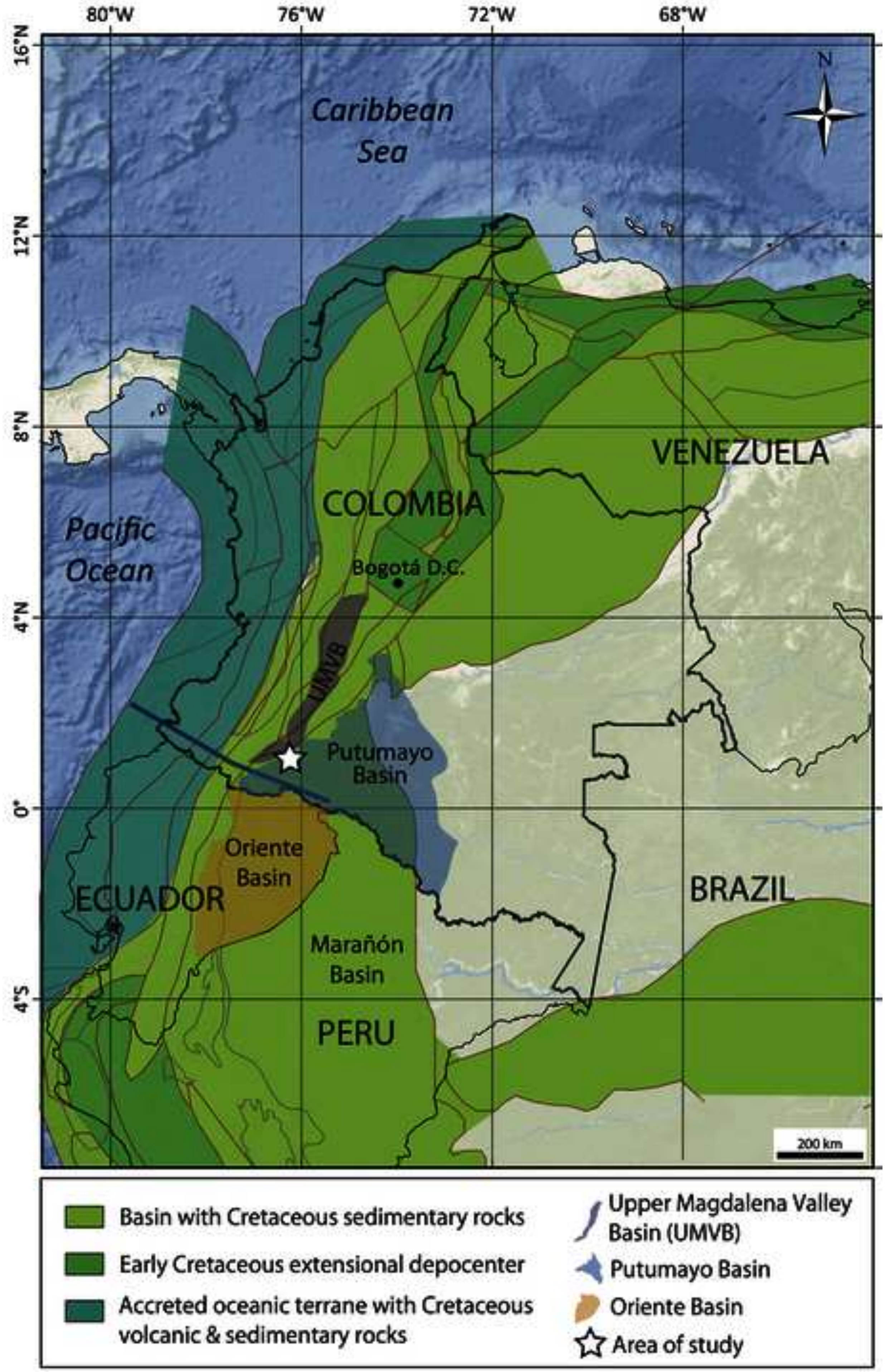

Figure 2

Click here to access/download;Figure;Figure 2_Strat Column_RR.jpg

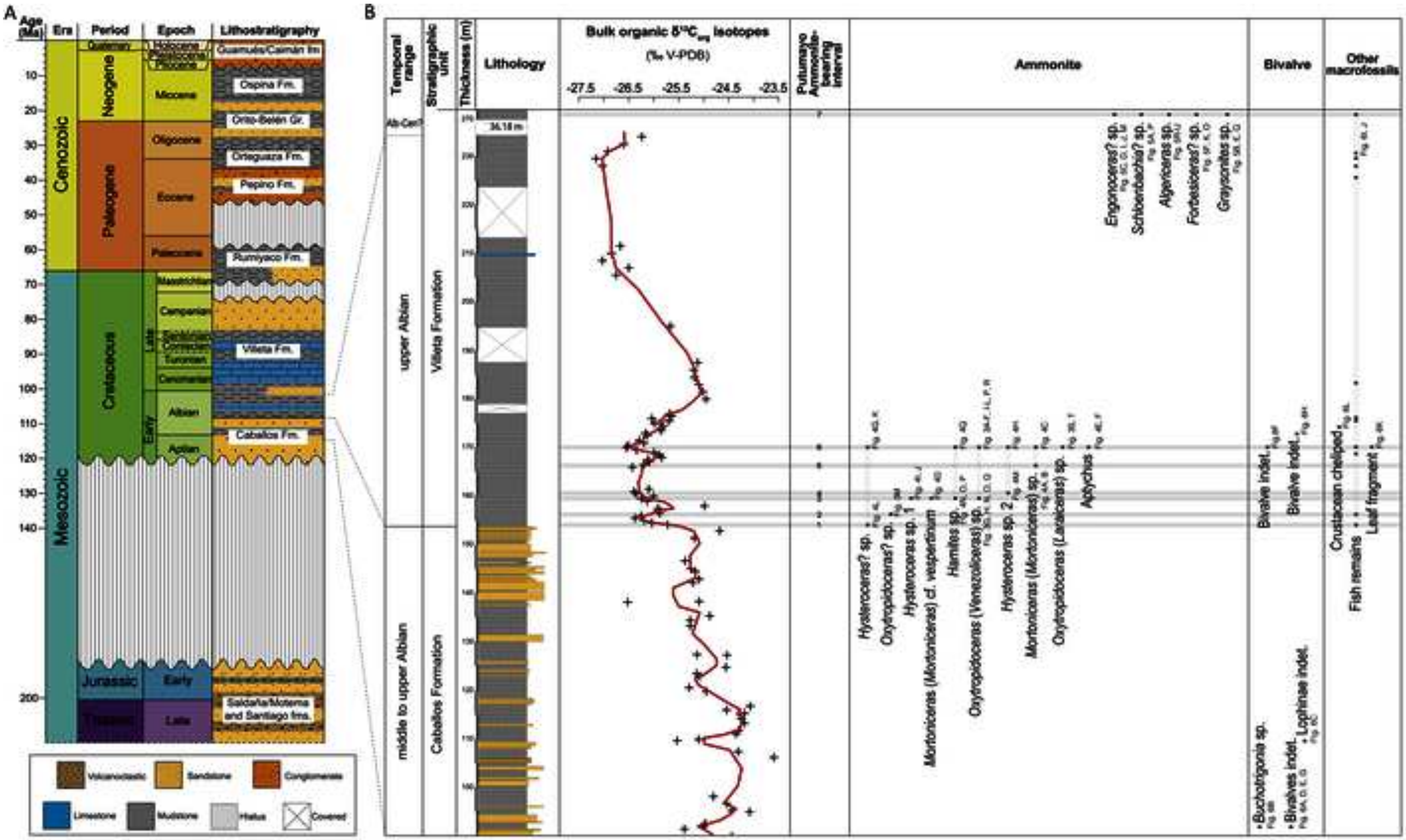

Figure 3

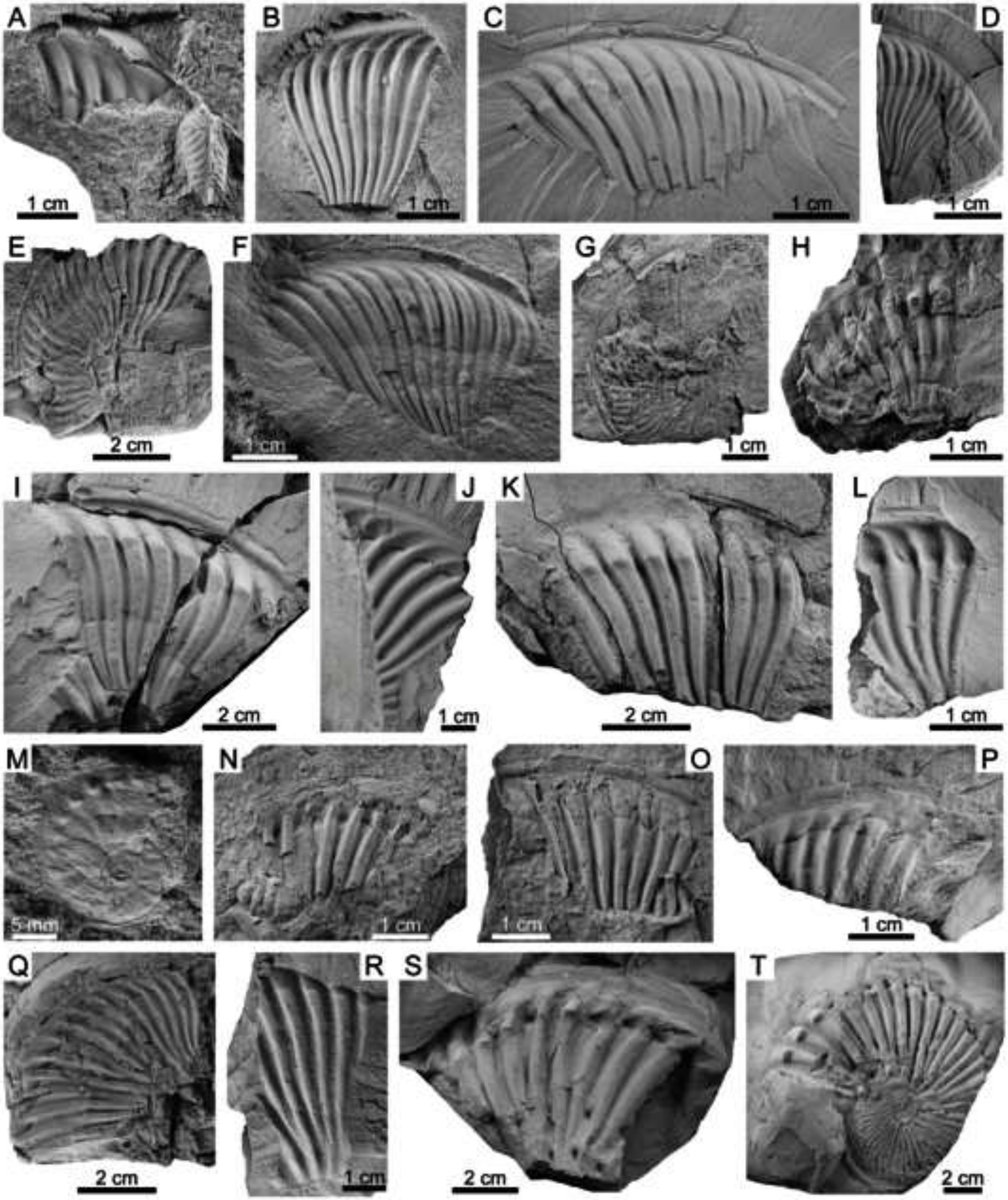

Figure 4

Click here to access/download;Figure;Figure 4_RR.png

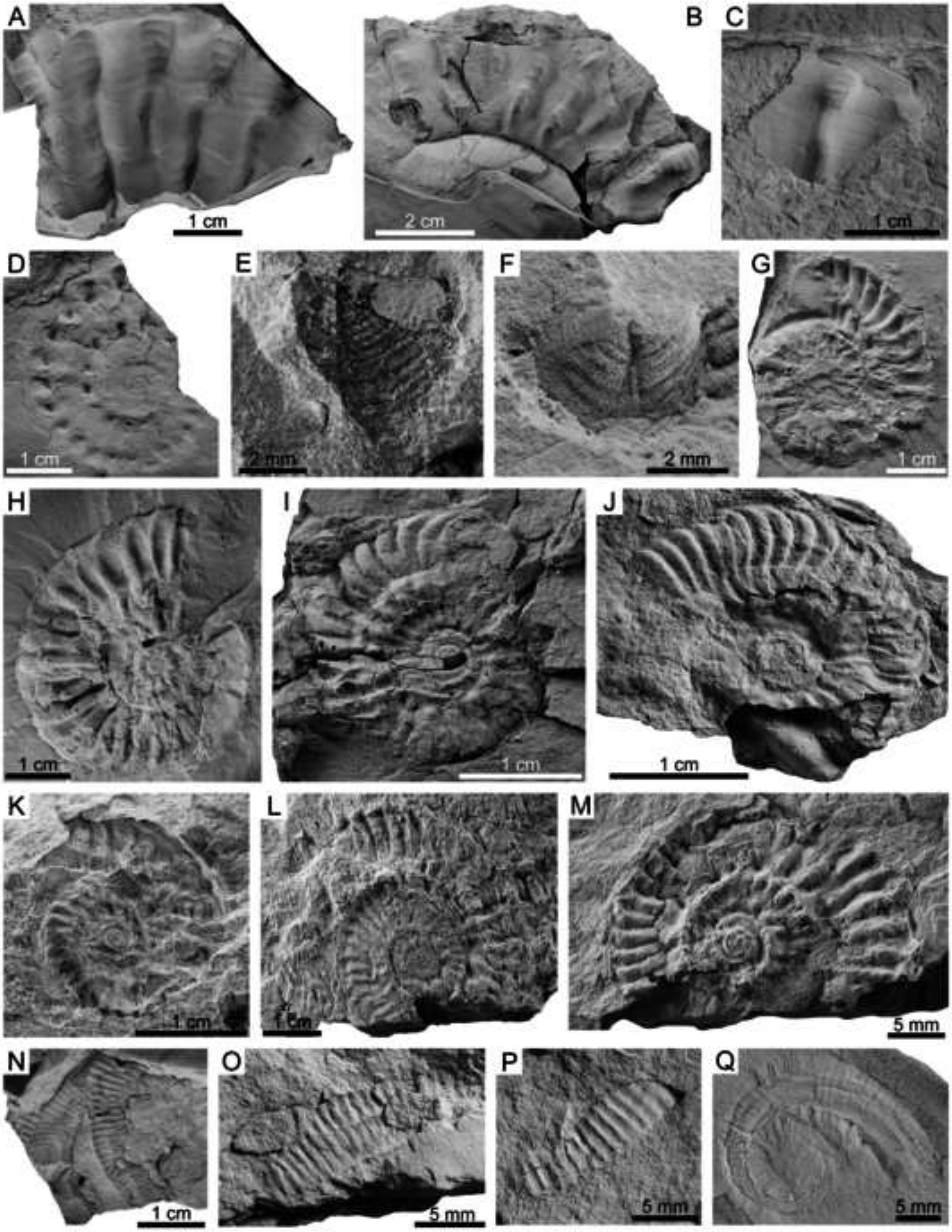

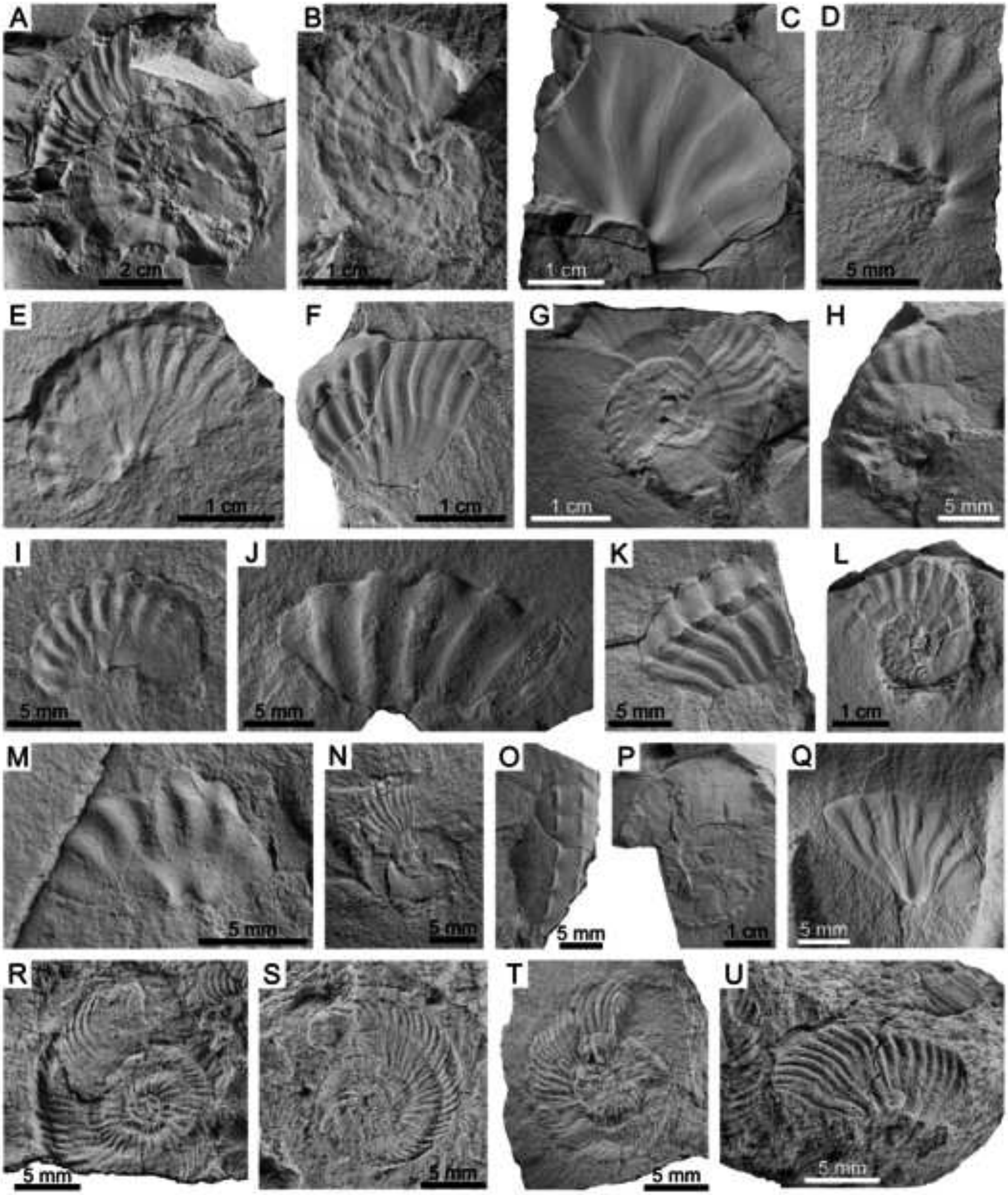
A
2 cm
B
1 cm
C
1 cm
D
5 mm
E
1 cm
F
1 cm
G
1 cm
H
5 mm
I
5 mm
J
5 mm
K
5 mm
L
1 cm
M
5 mm
N
5 mm
O
5 mm
P
1 cm
Q
5 mm
R
5 mm
S
5 mm
T
5 mm
U
5 mm

Figure 6 Click here to access/download;Figure;Figure 6_RR.png

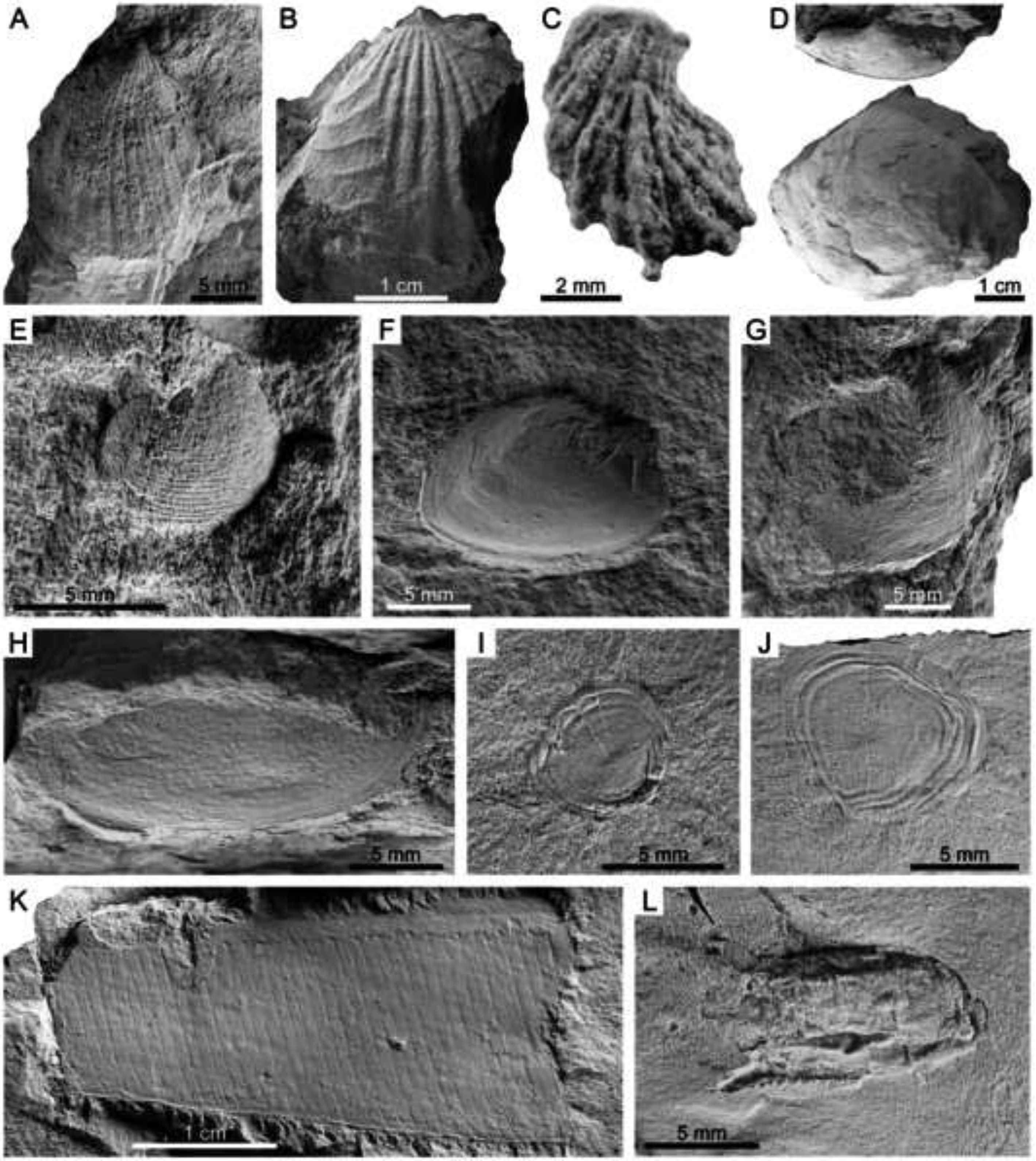

Figure 7

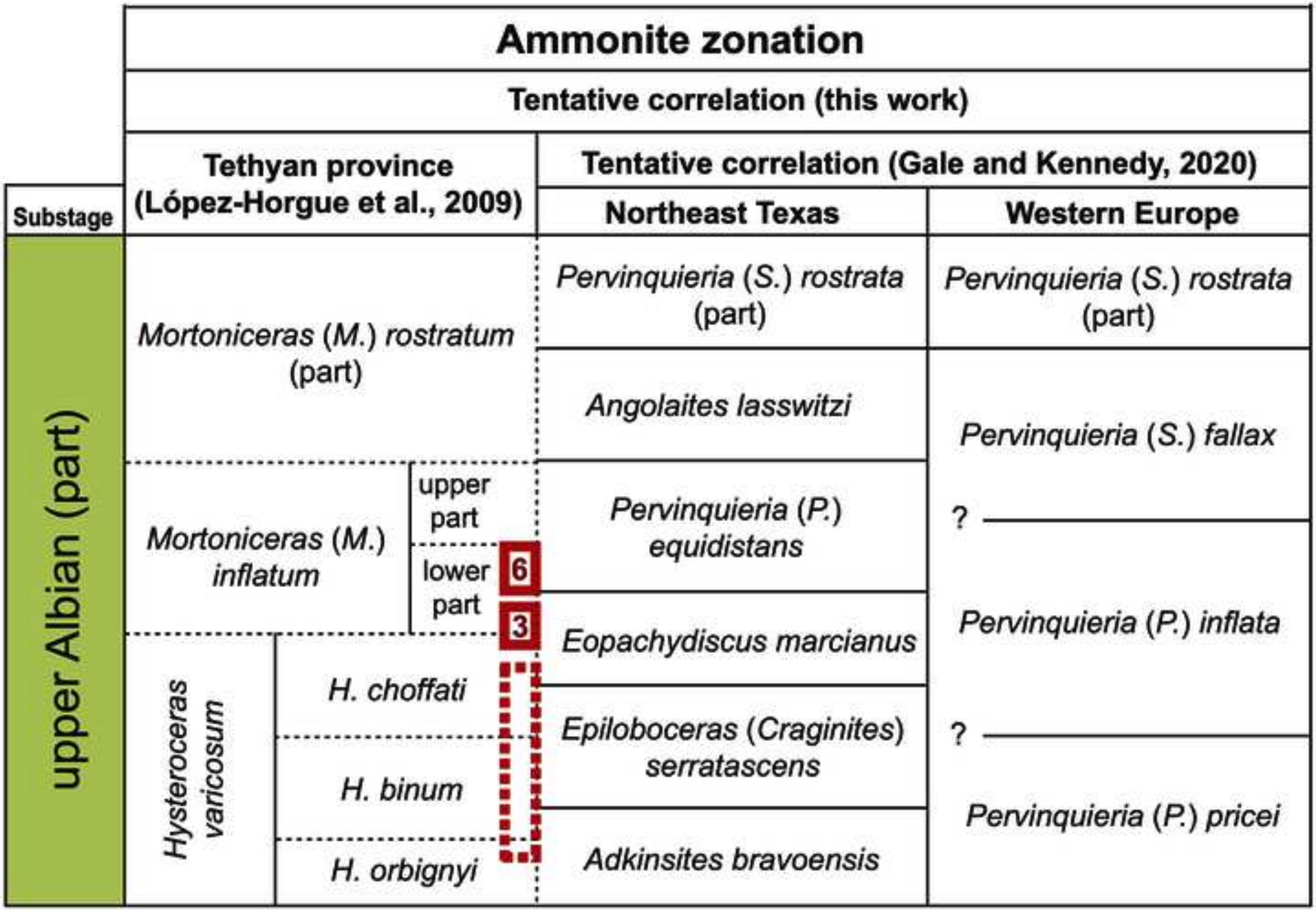
Ammonite zonation
Tentative correlation (this work)
Tethyan province (López-Horgue et al., 2009)
Tentative correlation (Gale and Kennedy, 2020)
Northeast Texas
Western Europe
Substage
upper Albian (part)
Mortoniceras (M.) rostratum (part)
Mortoniceras (M.) inflatum
upper part
lower part
6
3
Hysteroceras varicosum
H. choffati
H. binum
H. orbignyi
Pervinquieria (S.) rostrata (part)
Angolaites lasswitzi
Pervinquieria (P.) equidistans
Eopachydiscus marcianus
Epiloboceras (Craginites) serratascens
Adkinsites bravoensis
Pervinquieria (S.) rostrata (part)
Pervinquieria (S.) fallax
?
Pervinquieria (P.) inflata
?
Pervinquieria (P.) pricei

Figure 8

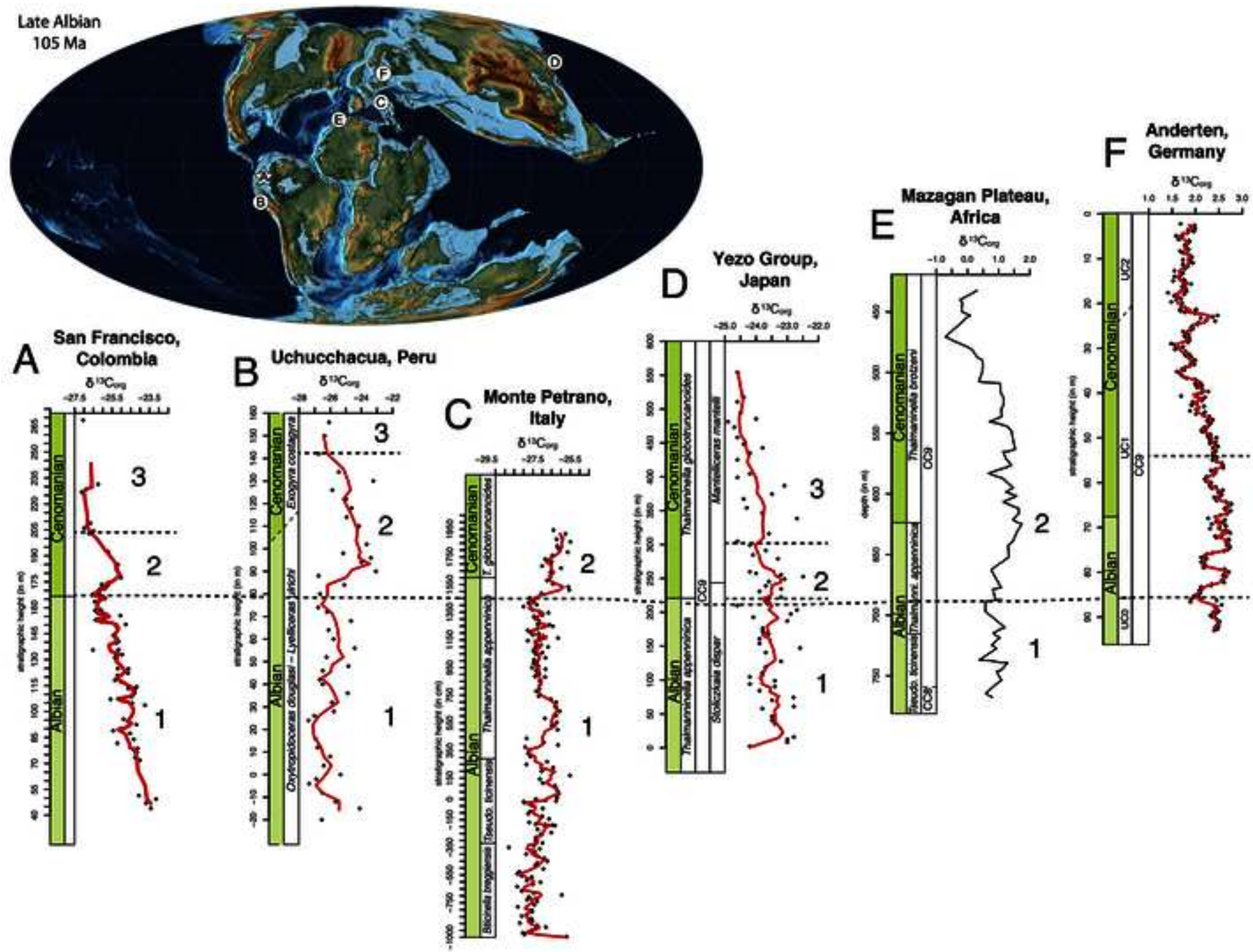
Late Albian
105 Ma
A
San Francisco, Colombia
B
Uchucchacua, Peru
C
Monte Petrano, Italy
D
Yezo Group, Japan
E
Mazagan Plateau, Africa
F
Anderten, Germany
Cenomanian
Albian
1
2
3